Detrital modes in sedimenticlastic sands from low-order streams in the Iberian Range, Spain: the potential for sand generation by different sedimentary rocks

José Arribas*, Amparo Tortosa

Departamento de Petrologia y Geoquimica, Facultad de Ciencias Geológicas, Universidad Complutense de Madrid, Madrid 28040, Spain

Abstract

The composition of modern stream sands derived from sedimentary source rocks in the Iberian Range has been analyzed in order to evaluate the contributions of the different bedrock types (mainly sandstones, limestones and dolostones). Temperate to subhumid climate and short transport conditions promote a weathering-limited denudation regime. As expected, sand composition proved to be essentially quartzolithic, with variable amounts of penecontemporaneous carbonates.

Sand compositional data were compared with the exposure areas of the different bedrocks in the drainage sub-basins considered for semi-quantitative assessment of the sand generation potential of each bedrock type. Siliciclastic formations (sandstones) appear to be by far the most significant sand producers, with Sand Generation Indices (SGIs) in the medium sand fraction ranging from 4 to 20; i.e., 4 to 20 times greater than the SGI of carbonate rocks. Composition and texture are the main factors controlling carbonate sand generation. Sparitic limestones yield higher SGIs (2.8 to 20) when source terrains are constituted exclusively by carbonate rocks. High sparite grain content in the sands is enhanced by supplies from additional sources, such as calcitized dolostones. Dolomicrite sources are strongly under-represented in the sands analyzed (very low SGI), whereas the proportion of micritic limestone grains tends to be an accurate reflection of that bedrock at the source.

Even though the results presented here refer to the first stage of sand generation with negligible transport effects, we think they may be helpful in the analysis and reconstruction of source terrains in ancient sedimenticlastic deposits.

Keywords: Sand; Provenance; Recycling; Sedimentary sources; Iberian Range; Spain

1. Introduction

Provenance analyses on sandstones attempt to solve one of the most complex questions relating to the origin of sands: the nature of the source area and subsequent modifications of erosion products. During the 1970s and 1980s, several models were developed to infer provenance from framework composition (e.g., Basu et al., 1975; Dickinson and Suczek, 1979; Dickinson, 1985; Valloni, 1985).

Subsequent studies concerned with modern sand compositions have played a crucial role in testing and improving traditional models and interpretation schemes by providing the possibility of a direct comparison between source system settings and composition of the sandy products (Ibbeken and Schleyer, 1991; Palomares and Arribas, 1993; Montesinos and

* Corresponding author.
E-mail address: arribas@geo.ucm.es (J. Arribas).

Arribas, 1998; Arribas et al., 2000; Le Pera et al., 2001). In fact, actualistic studies can largely isolate the effects of the many closely interrelated parameters involved in the genesis of clastic sediments, including source-rock composition, climate, weathering and transport (Johnsson, 1993).

Head stream sediments represent the product generated first in a fluvial system, with source lithology the dominant influence and with little or negligible modification caused by transport processes (mechanical breakdown, hydrodynamic sorting) (e.g., Basu, 1985). In order to evaluate the potential of different bedrock types for producing sand in head streams, the concept of the Sand Generation Index (SGI) was introduced by Palomares and Arribas (1993). The SGI of a given bedrock type A of a dual source A+B is expressed in terms of the outcrop area (in percentage) of A ($\%S_A$) required to produce a sand whose modal composition represents the average between the modes of sands derived from pure A and B sources (Palomares and Arribas, 1993). Values of SGI are expressed as $100/\%S_A$. Thus, an equal potential to produce sand between A and B bedrock types means a SGI equal to 2 for both bedrocks. This made it possible to evaluate quantitatively the relative capability of bedrock types to generate sand in a crystalline source terrain (granitoid+gneiss; gneiss+slate-schist and granitoid+slate-schist bedrock associations).

However, little is known so far about the potential of the different sedimentary rock types to produce clastic sediments. The origin of sedimenticlastic deposits is related to recycling processes, the relevance of which in the genesis of detrital material has been stressed by several authors (Blatt and Jones, 1975; Garrels, 1986). In addition, petrographic criteria have been established to detect sediment recycling (Folk, 1974; Zuffa, 1987; Arribas et al., 1990). The first attempts at quantitative assessment of the relationship between sedimentary source settings and sand composition were made by Mack (1981), Grantham and Velbel (1988) and Ibbeken and Schleyer (1991), among others.

The purpose of this study is to compare the composition of sedimenticlastic sands in head streams with different proportions of the specific sedimentary rocks constituting the source terrains. The study area is located in the Iberian Range (Central Spain), where a wide variety of Mesozoic carbonates and sandstones are eroded in catchment areas under temperate to subhumid climatic conditions. Several small-scale drainage sub-basins (<30 km^2) were selected, where variables such as climate and transport effects can be considered constant or of negligible influence on sediment composition. A quantitative analysis of the source terrains, using a geographical information system, permitted a detailed comparison of bedrock characteristics (lithology, exposure area) with the corresponding sand composition and hence the evaluation of the relative potential for sand generation of the different sedimentary source rock types. The results may help provide a better understanding of detrital modes of sedimenticlastic deposits, especially in Tertiary basins associated with the Alpine chains in the Mediterranean area.

2. Study area

The Iberian Range is an Alpine mountain chain, about 400 km long with a northwest–southeast trend, where Mesozoic sedimentary rocks overlying Variscan basement are widely exposed. Sedimentation during the Alpine cycle was initiated in a continental rift/aulacogen setting and evolved into a double vergent chain due to compressive deformation from Upper Cretaceous to Upper Oligocene (Alvaro et al., 1979). The drainage areas considered in this paper are located in the northwestern sector of the Iberian Range (NE of the city of Cuenca), covering about 2500 km^2 (Fig. 1). In this area, the Mesozoic stratigraphic record consists of a sedimentary succession up to 2600 m thick. However, Triassic formations (about 1000 m thick) are poorly represented in the drainage basins selected, with the uppermost lutitic–evaporitic terms of the Keuper (Germanic facies) outcropping only locally. Jurassic units are represented by approx. 750 m of shallow-marine limestones with mud-supported and subordinately grain-supported textures, and dolostones. Arkoses and subarkoses prevail in the Lower Cretaceous section (300 m thick). Finally, the Upper Cretaceous strata (about 550 m) are dominated by dolomitic lithologies, mainly dolosparite (Vilas et al., 1982). Dedolomitization processes have been reported from this interval (Fernández Calvo, 1981). Locally, modern travertine carbonate deposits appear associated

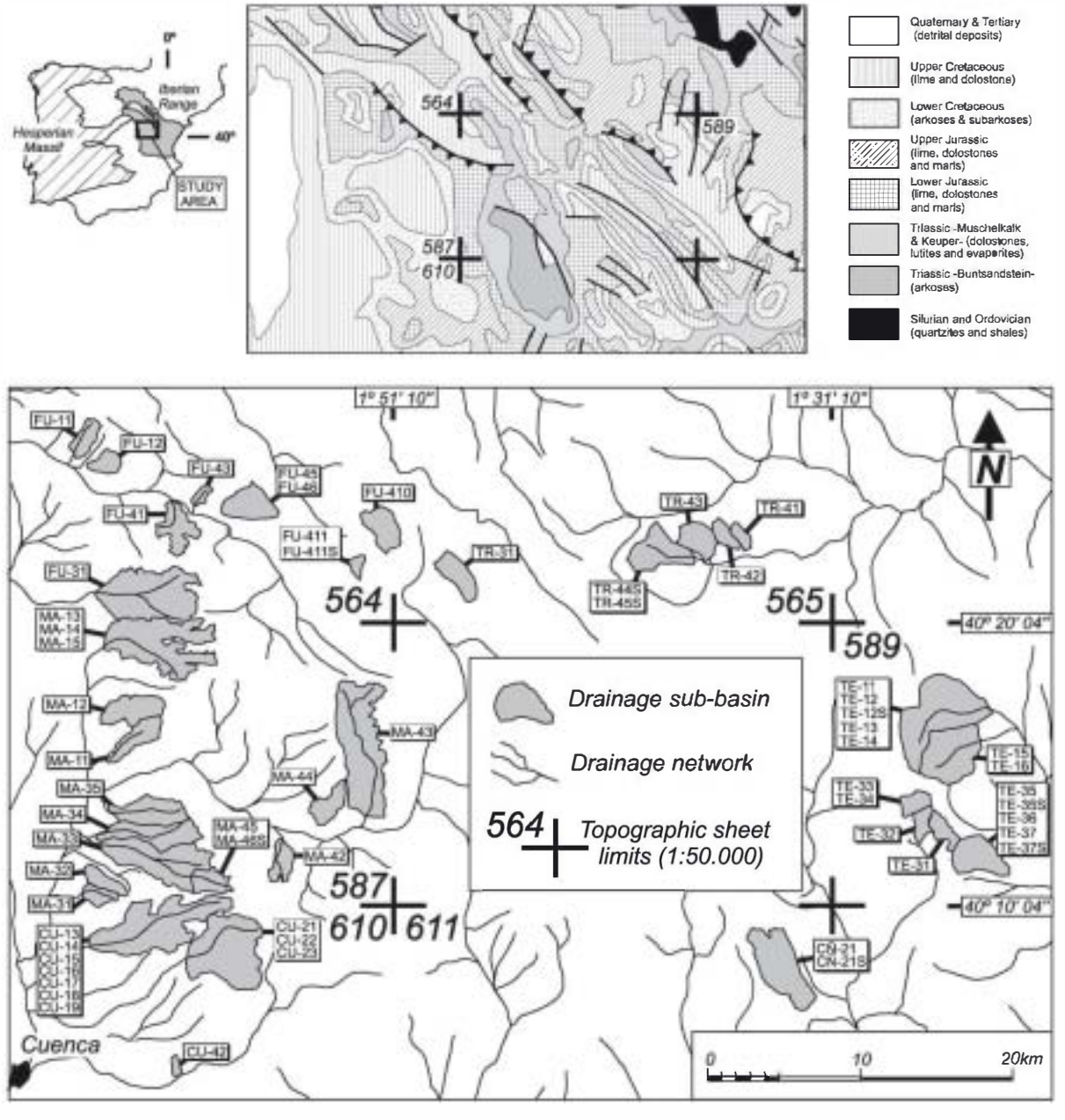

Fig. 1. Generalized map of the study area and location of samples.

with main streams, acting as a coeval carbonate source of detritus.

The study area is characterized by a temperate to subhumid climate with warm summers and no dry seasons (Cfb of Köppen, 1901). Mean annual precipitation ranges from 500 to 800 mm and mean annual temperatures range from 8° to 12° (I.G.N., 1991a). Thus, both mechanical and chemical weathering can be assumed to be moderate according to Wilson (1969). Soils are thin, poorly developed and consist mainly of inceptisols identified as cryochrepts, ustochrepts and xerochrepts (I.G.N., 1991b). Vegetation

cover is characterized by predominantly hardwood and pine ecosystems (*xerofilum*, *perennifolium* and *esclerofilum*).

Human pressure on the area studied is very low, without any notable influence on sedimentary processes. Locally, deforestation has generated meadows in the lower parts of drainage basins along the river courses. Depopulation has resulted in negligible human activity (no industrial settlements and scant agriculture). Activity in the pine and hardwood forests is limited and consists of controlled pine felling.

The drainage sub-basins studied are elongated in shape, following the main Alpine structural trends of the Iberian Range (E–W, N–S and NW–SE trends). The areas occupied by these basins range from 2 to 20 km^2 and all of them exhibit drainage networks at a similar stage of evolution, mainly constituted by first- and second-order streams. Drainage divides range from 1000 m to 1840 m in altitude, and mean slope values vary between 15% and 35%. Water courses mainly have a seasonal regime, running during winter and spring with occasional inputs from springs. Detailed characteristics of the drainage sub-basins are shown in Fig. 2.

Channels in the highlands of the drainage areas are narrow (5 to 20 m wide) and cut deep into the bedrock (Fig. 3A). In these areas, gravel deposits prevail, exhibiting a chaotic arrangement due to local supplies from steep slopes. Channel width increases downstream (30 to 100 m) and sandy gravel carpets and bars (longitudinal and small pointbars) develop (Fig.

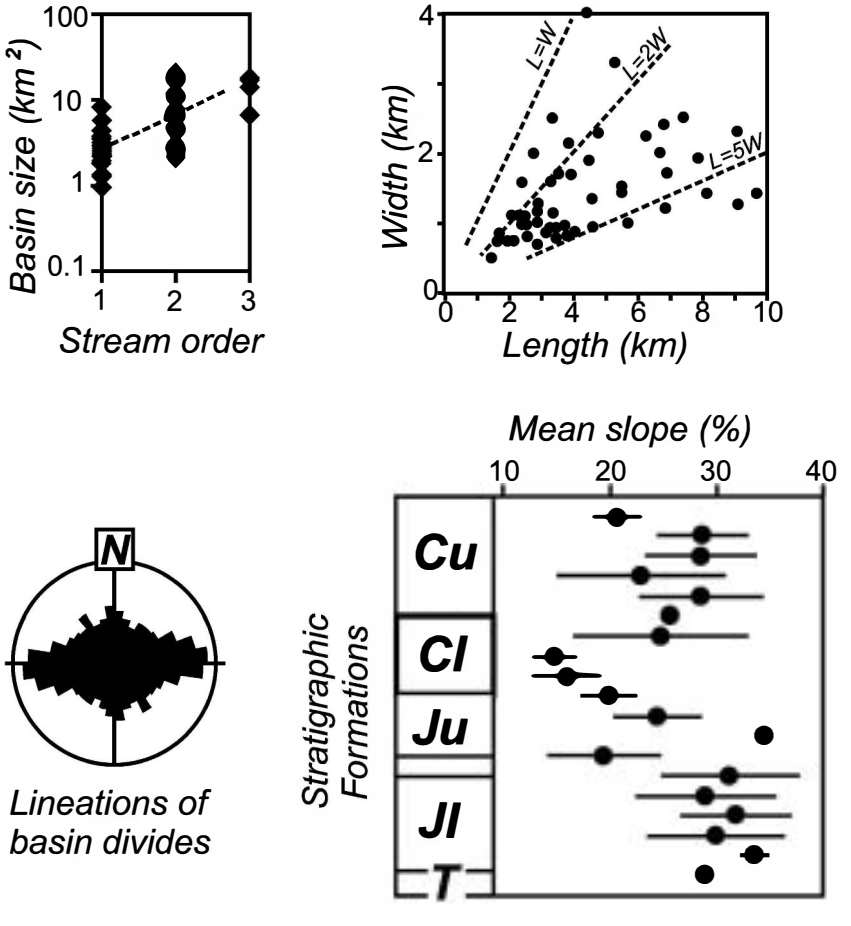

Fig. 2. Physiographic characteristics of analyzed drainage basins. T: Triassic; Jl: Lower Jurassic; Ju: Upper Jurassic; Cl: Lower Cretaceous; Cu: Upper Cretaceous.

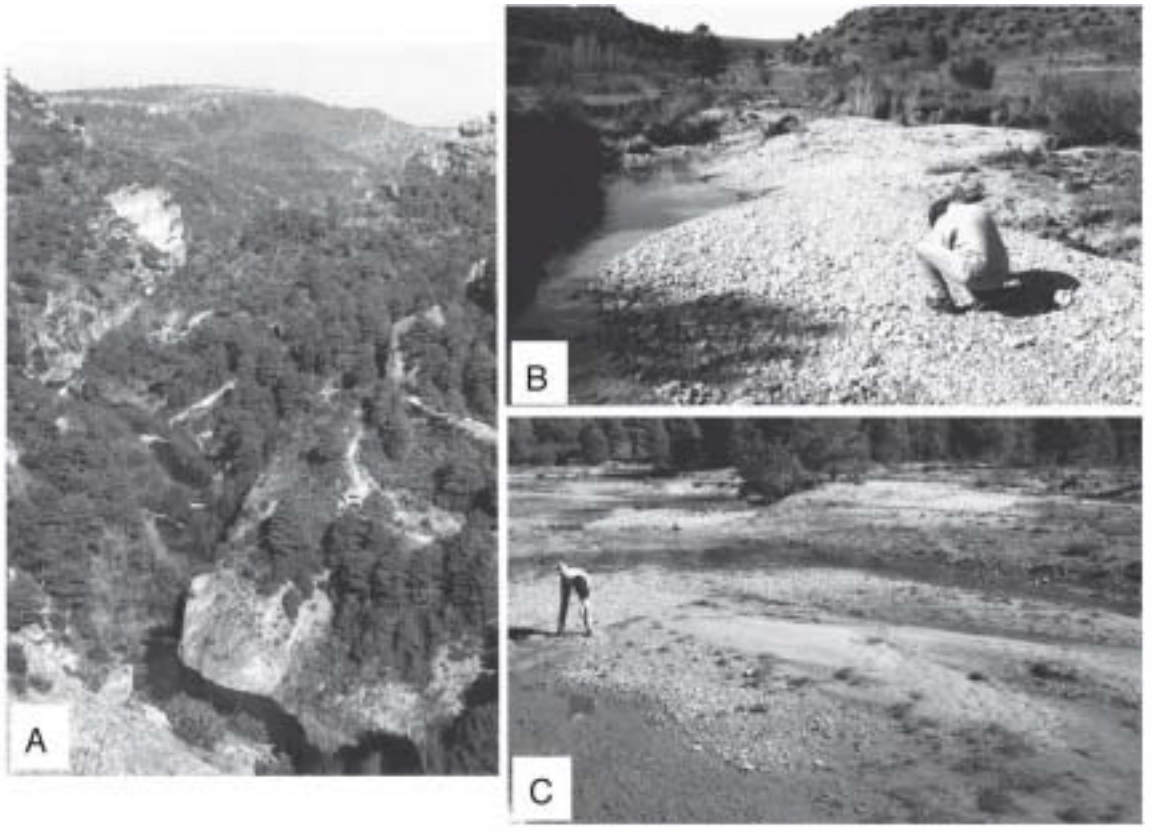

Fig. 3. (A) General view of the Júcar River head stream cutting carbonate bedrock. (B) Sandy gravel longitudinal bar from the Encabas River. (C) Sand bar developed on a gravel carpet in the inner part of the Encabas River. Notice lateral gravel deposits in the incipient alluvial plain.

3B). Sand deposits occur as drift deposits behind obstacles (pebbles, cobbles and plants) generated by flooding of incipient alluvial plains, or even within the main channels (Fig. 3C). All these deposits may be classified as first-order of sampling (Ingersoll et al., 1993), and their composition reflects a dominant influence of bedrock types.

3. Methods

3.1. Sampling and petrographic methods

A total of 60 samples were collected from 35 drainage sub-basins (Fig. 1). Each sample consisted of 2 to 3 kg of detrital material of less than 20 mm grain size. All samples were washed and dry sieved at 1Φ intervals. Sand composition was analyzed in three sieved grain-size fractions: coarse (1–0.5 mm), medium (0.5–0.25 mm) and fine (0.25–0.125 mm) sand. Subsamples of each of these fractions were impregnated with epoxy resin for thin-sectioning. Thin sections were stained using alizarine (Evamy, 1963) and sodium cobaltinitrite (Chayes, 1952) solutions to facilitate identification of carbonate and feldspar, respectively. The modal composition was determined by point counting following the criteria established by Gazzi (1966) and Dickinson (1970). The use of grain types corresponding to the so-called 'traditional' criteria (Ingersoll et al., 1984) can be considered by re-evaluation of the point-count results. Two hundred to 400 grains were counted per thin section and classified into 56 modal classes (Table 1 and Appendix A). Differences in the number of grains counted are due to the availability of material in each sample fraction.

Table 1
Sand petrographic parameters

SG (single grains)	AN (ancient non-carbonates)	Qm	Qs	Monocrystalline quartz	
			Qp	Polycrystalline quartz (subgrains >0.062 mm)	
			Qi	Quartz with evaporite inclusions	
			Qr	Quartz in rock fragment	
		F	Ks	K-feldspar (single grain)	
			Kr	K-feldspar in rock fragment	
		L	Mf	Mudrock fragment	
			Ch	Chert	
			Mc	Mica	
			Mr	Mica in rock fragment	
			Ot	Others (mainly heavy minerals and Fe-oxides)	
			Sc	Carbonate cement in sandstone	
			Sf	Ferruginous cement in sandstone	
			Sm	Phyllosilicate matrix in sandstone	
	AC (ancient carbonates)	CAL	Lm	Micrite	Lmwp
			Lw	Wackestone	
			Lp	Packstone	
			Lg	Grainstone	Lgec
			Le	Sparitic limestone	
			Lc	Calcite single crystal	
			Fo	Fossil	
			Ls	Sandy limestone	
		DOL	Dm	Dolomicrite	
			De	Dolosparite	Dr
			Dc	Dolomite single crystal	
			Dd	Dedolomite	
			Ds	Sandy dolomite	
	PC (penecontemporaneous carbonates)		Bio	Bioclast	
			In	Algal- and plant-induced carbonate grain	
CG (compound grains)	= SG + Coeval carbonate coating		X(SG)	All above classes with coeval carbonate coating	
			En	Coeval carbonate coating	
	Other petrographic parameters				
	Lt = L + AC				
	Q = Qm + Ch				

3.2. Petrographic categories

The petrographic database (Appendix A) is constituted by two main grain types: (1) single grains, consisting of any type of grain whose composition is related to only one source, and (2) compound grains, which have a nucleus of clastic material (single grain) with a coeval carbonate coating. The presence of compound grains is closely related to the presence of penecontemporaneous carbonate grains. Single grain types comprise six subgroups with a total of 28 petrographic classes, defined by their textures and composition (Table 1). Based on the nature of their nuclei, an equivalent number of petrographic classes of compound grains are considered (X(SG) in Table 1 and Appendix A). Following Gazzi–Dickinson criteria, if the cross-hair fell on the nucleus that point was counted as a type of compound grain with an AN, AC or even PC nucleus (X(SG) types); if it fell on the carbonate coating this point was counted as 'En' (Table 1).

3.2.1. Ancient non-carbonates (AN)

This subgroup mainly comprises siliciclastic monomineral (quartz, K-feldspar, micas, and heavy minerals) and polymineral grains with microcrystalline textures (i.e., lutitic grains) and coarse grained rock fragments. Monomineral grains are more abundant than either fine- or coarse-grained rock fragments. Polycrystalline quartz occur as clasts with coarse subgrains (>0.062 mm) or as chert grains

(aggregates of cryptocrystalline quartz). The predominant coarse-grained fragments are sandstones with sparitic carbonate or ferruginous cement and clay matrix. The coarse-grained rock fragments were counted as the monomineral component beneath the cross-hair (Qr, Kr, Mr, etc.). The AN subgroup is equivalent to NCE grains defined by Zuffa (1980).

3.2.2. Calcitic components (CAL)

These have micritic (Lmwp in Table 1) and sparitic (Lgec) textures. Micritic microfacies identified include micrite (Lm), wackestone (Lw) and packstone (Lp). Sparitic grains consist of coarse crystalline limestone fragments (Le) and monocrystalline calcite grains (Lc). Clasts with grainstone microfacies (Lg) are also classed as 'sparitic grains', as they contain abundant sparitic cement. Echinoderm and pelecypod fragments are frequent as isolated fossils (Fo). Finally, limestone fragments with variable content of siliciclastic components (Ls) have been identified.

3.2.3. Dolomitic components (DOL)

These consist of dolostones grains with similar textures to the calcitic microfacies described above (Dm, De, Dc and Ds). Dw, Dp and Dg categories are not recognized as sand grain microfacies. Grains with dedolomitization textures (Dd) are also very frequent in some deposits.

Both CAL and DOL subgroups are equivalent to AC (ancient carbonate) grains as defined by Cavazza et al. (1993), and to CE of Zuffa (1980).

3.2.4. Penecontemporaneous carbonates (PC plus En)

These encompass a wide variety of carbonate grains with micritic and sparitic textures and characterized by the presence of fine algal microstructures, as described in continental carbonates by Freytet and Verrecchia (1998). In addition, some grains lacking these features, but with irregular borders and constituted by a 'spongy' micrite, have been included in this category (In). Their origin is associated with the erosion of travertine deposits and freshwater carbonate concretions (Arribas and Tortosa, 1998; Freytet and Verrecchia, 1998; Pedley, 1990). Bioclasts (Bio) are scarce, appearing locally as fragments or as well preserved gastropod shells.

In addition, compound grains (CG in Table 1) show coeval micritic coatings growing over a nucleus. These thin coatings are structureless, in some cases presenting a succession of concentric micritic bands. Counted points from these coatings have been included in the 'En' petrographic class. Nuclei of compound grains may be included in any of the petrographic categories described above.

3.3. Quantification of source area geology

In order to evaluate the effect of source area on the composition of the sandy deposits, a source-area database comprising the main physiographic and lithologic characteristics of the catchment area was constructed. The sub-basin of each sand sample was considered to comprise the portion of drainage basin that is uphill from the sample site. A geographical information system (ILWIS, version 1.4) was used to build the data base (Appendix B). Geological information regarding the percentages of outcrop area of the different cartographic units in the sub-basins was acquired from geologic maps at 1:50,000 scale (I.T.G.E., 1983a,b, 1986, 1989a,b,c) and transformed by digitizing into polygon and raster map formats. Slope data were obtained from a digital elevation model generated by digitization of topographic maps (scale 1:50,000). Tables with the outcrop area and the related slope data of each cartographic unit are created by combining pixel values ('crossing') of both geological and slope raster maps (Montesinos and Arribas, 1998). Often, digitized cartographic units from geologic maps comprise more than one lithology. However, these cartographic data have been transformed into lithologic-type percentages by using additional information from map memoirs and unpublished complementary data (cross sections, petrographic data and detailed descriptions). This transformation has been applied to each geological sheet (scale 1:50,000) being applicable only to the sub-basins occurring in that sheet. Table 2 illustrates an example of this transformation (sheet no. 564). The authors can provide transformations from the other sheets on request. In some cases, the lithologic information has proved to be scarce, and detailed compositional data are lacking. We thus distinguished broad but simple lithologic groups: micritic limestone (Lmwp); sparitic limestone (Lgec); fine-crystalline dolostones (Dm); medium- to coarse-crystalline dolostones (Dr); siliciclastics (AN) and marls

Table 2
Lithofacies of the cartographic units from sheet no. 564 (Fuertescusa), used for transformation of cartographic data into lithologic parameters of sub-basins in sheet no. 564

Fuertescusa (no. 564)											
	Cartographic units			Lithofacies (%)							
				Lm[a]	Lw[a]	Lp[a]	Lg[a]	Dm[a]	Dr[a]	AN[b]	Mar[c]
Cretaceous	Cu	13	Fm. Brechas dolomíticas de Cuenca				10		90		
		12	Fm. Calizas dolomíticas del Pantano de la Tranquera						100		
		11	Fm. Dolomías de la Ciudad Encantada				25		75		
		10	Fm. Margas de Chera; Fm. Dolomías de Alatoz; Fm. Dolomías de Villa de Vés; Fm. Margas de Casa Medina.					21	49		30
	Cl	9	*Facies Weald*; Fm. Arenas de Utrillas		3					89	8
		8	Fm. Arenas de Utrillas							100	
		7	*Facies Weald*		10					70	20
Jurassic	Jm	6	Fm. Carbonatada de Chelva	50	50						
	Jl	5	Fm. Margas y Calizas de Turmiel								100
		4	Fm. Margas del Cerro del Pez; Fm. Calizas bioclásticas de Barahona	50	50						
		3	Fm. Calizas y Dolomías de Cuevas Labradas	8	8		5		79		
Triassic/Jurassic	J/T	2	Fm. Dolomías tableadas de Imón; Fm. Carniolas de Cortes de Tajuña					50	50		

Jl: Lower Jurassic; Jm: Middle Jurassic; Cl: Lower Cretaceous; Cu: Upper Cretaceous.
Source of information: Complementary data of the 564 sheet, Instituto Tecnológico y Geominero de España (I.T.G.E.).
[a] See Table 1 for explanation.
[b] Siliciclastics (mainly conglomerates and sandstones).
[c] Marls.

(Mar). Transformation of cartographic units into lithologic groups can be expressed as a matrix multiplication:

$$Lx = \begin{vmatrix} lg_{11} & lg_{12} & \dots & lg_{1n} \\ lg_{21} & lg_{22} & \dots & lg_{2n} \\ \dots & \dots & \dots & \dots \\ lg_{m1} & lg_{m2} & \dots & lg_{mn} \end{vmatrix} \cdot \begin{vmatrix} CU_1 \\ CU_2 \\ \dots \\ CU_n \end{vmatrix} = \begin{vmatrix} LG_1 \\ LG_2 \\ \dots \\ LG_m \end{vmatrix} : 100$$

where, lg_{mn} is the percentage of the m lithologic group that is represented in a given n cartographic unit; CU_n is the area (%) of the n cartographic unit from the x sub-basin; and LG_m the percentage of representation of the m lithologic group in the x sub-basin. The final source lithology database for the sub-basin involved in the genesis of each sample is shown in Appendix B. Travertines and other recent carbonate formations appear to be associated to stream courses and are not represented on 1:50,000 scale geologic maps. Thus, quantification of recent carbonate sources was not possible, and so Appendix B refers only to ancient bedrocks.

4. Stream sand composition

Modal sand composition in fine, medium and coarse grain-size intervals varies considerably, from nearly pure siliciclastic sand to nearly pure carbonate-rock-fragment sand (Fig. 4). Penecontemporaneous carbonates (PC plus En) do not generally exceed 25% of total grain population. These variations in sand composition reflect a wide variety of sedimentary sources in the different sub-basins and the productivity of those sub-basins as coeval carbonate sources. Occasionally, penecontemporaneous carbonate content exceeds 90% of the bulk sediment, causing considerable dilution of non-carbonate (AN) and carbonate-rock-fragment grains (AC) supplied by the source rocks. The concentration of penecontemporaneous carbonates in fine, medium and coarse grain size fractions is shown in Fig. 4.

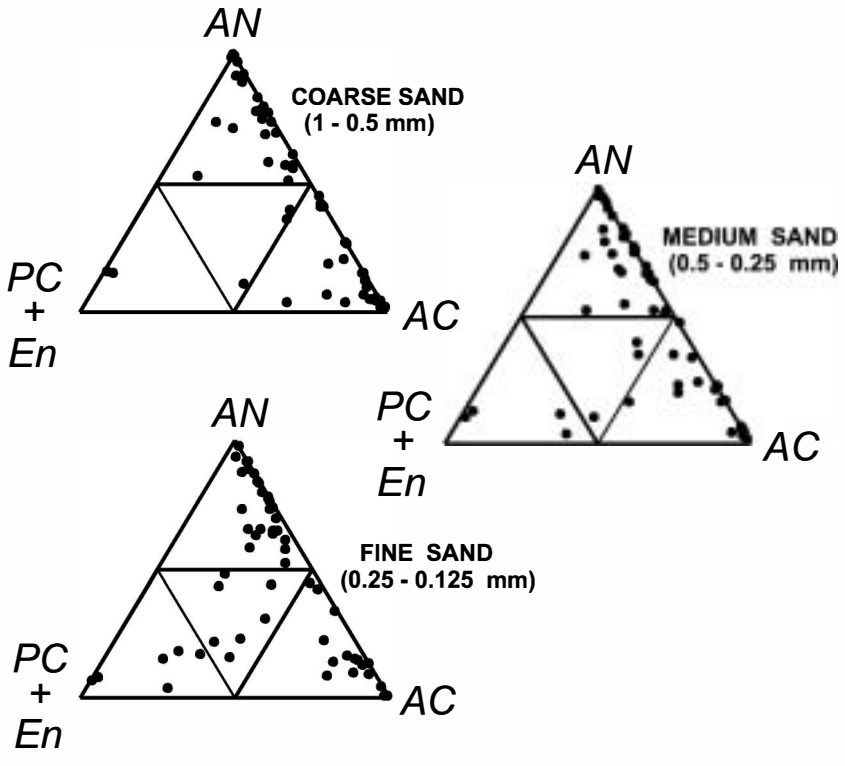

Fig. 4. Ternary diagrams of relative proportions of ancient non-carbonates (AN), penecontemporaneous carbonates (PC + En) and ancient carbonates (AC) grains for coarse, medium and fine sand fractions of low order stream deposits from the Iberian Range.

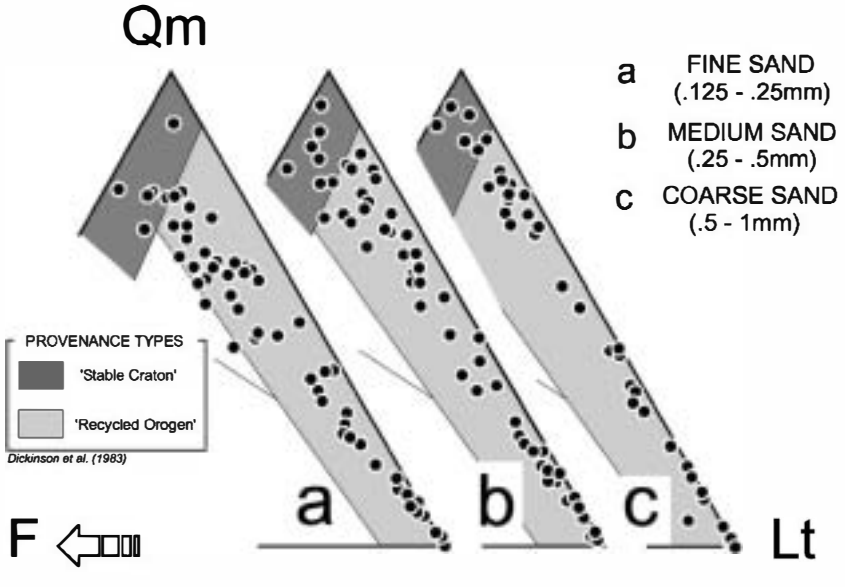

Fig. 5. QmFLt ternary diagrams for coarse, medium and fine sand fractions of low order stream deposits from the Iberian Range. For explanation of petrographic indices, see Table 1.

Sands are quartzolithic in composition, plotting near the QmLt line on a QmFLt diagram (Fig. 5) and, as expected, reflecting a 'recycled orogen' provenance (Dickinson et al., 1983), but with clear dependence of sand composition on grain size. The high concentration of Qm grains in some samples produces a shift to the 'stable craton' field (Dickinson et al., 1983). This apparent inconsistency can be explained by the short-distance displacement of these deposits (first scale of sampling in Ingersoll et al., 1984), so that the original composition of the bedrock (arkoses and subarkoses) is maintained with little compositional changes in the recycled sand. Temperate climatic conditions mitigate chemical weathering and also favour feldspar preservation. Also visible is the concentration trend of feldspar when grain size diminishes (Odom et al., 1976).

The presence of the different types of carbonate rock fragment also differs if we compare their concentrations in the three grain size fractions (Fig. 6). Thus, the fine fraction is rich in dolospar grains (dolosparite -De- and dolomite single crystal -Dc- grains), containing nearly 50% more than the medium or coarse fractions. On the other hand, there are 30–50% less micritic grains (Lmwp and Dm grains) in the fine than in the coarse fraction. Sparitic limestones present a similar trend to micritic carbonate grains, but less pronounced. This suggests that that limestone grains are more stable in coarser fractions and that micritic microfacies are the least stable microfacies in the fine sand fraction.

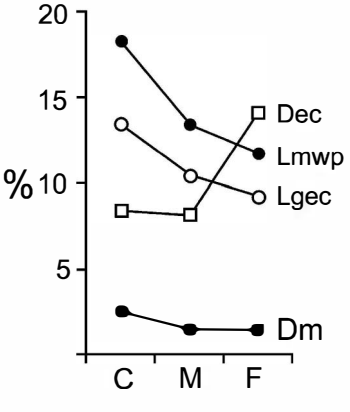

Fig. 6. Mean percentage of different carbonate grain types for coarse, medium and fine sand fractions of low order stream deposits from the Iberian Range. Dec: dolosparitic grains. Dm: dolomicritic grains. Lgec: sparitic limestone grains. Lmwp: micritic limestone grains.

5. Source vs. sand contrast

As a first approach to comparing drainage basin characteristics and petrography of sediments, we used the petrographic classes described earlier: (1) AN (ancient non-carbonates), (2) CAL (limestone grains) and (3) DOL (dolomitic grains). These groups can be checked against data relating to the surface distribution of siliciclastic, calcitic and dolomitic formations, respectively, in the source. AN-CAL-DOL ternary diagrams (Fig. 7) provide relevant information about the capability of a specific setting of sedimentary lithologies to produce sandy deposits. To facilitate comprehension of the contrast, sub-basins have been arbitrarily grouped according to the percentage of surface occupied by dolostone (100% to 85%, Fig. 7a; 85% to 45%, Fig. 7b; and 45% to 0%, Fig. 7c). By classifying samples in this way, we were able to work with relatively homogeneous groups of samples generated from similar bedrock distributions at the sources. In addition, these groups contain similar numbers of samples. Compositional data of coarse, medium and fine sand fractions are shown in Fig. 7, classified by the mean and the 95% confidence level polygon. As expected, there is not a one-to-one ratio between percentages of lithologies in a source area and the percentage of their products in the sediment. This is taken to be a consequence of the different potential of different sedimentary source rocks to produce sand. Surprisingly, sources constituted predominantly by dolomitic bedrocks (Fig. 7a) generate sands where calcitic grains predominate over dolomitic grains, mainly in the coarse and medium sand fractions. The richness of sediments in calcitic components with respect to the total carbonates may be related to dedolomitization processes acting in dolostone formations. Non-carbonate (AN) and calcitic (CAL) grains appear over-represented in the sand, and as a result, the quantitative information about dolomitic occurrence in the source is drastically reduced. The composition of the fine sand fraction differs slightly from the coarser fraction, having a higher concentration of dolomite grains. There is also loss of dolomite representation in the sand when the presence of dolostones in the source

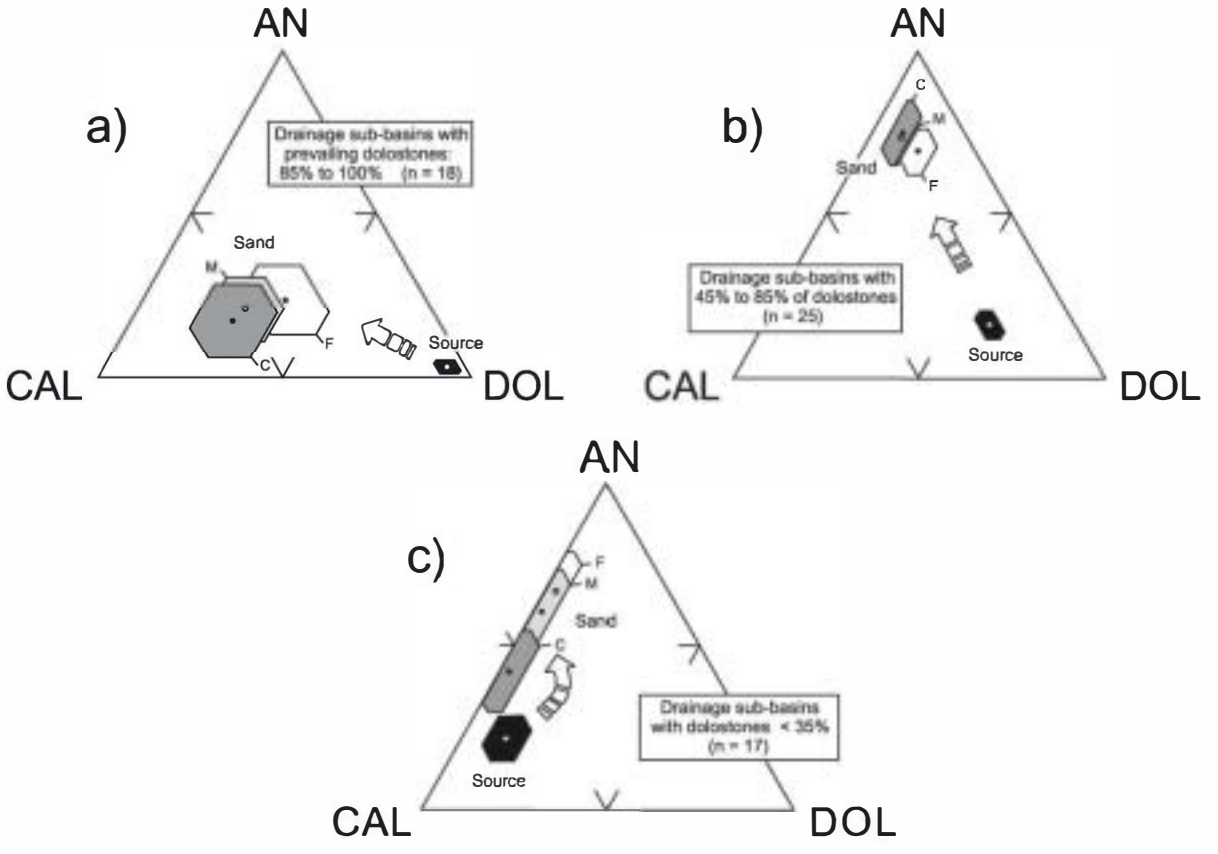

Fig. 7. AN/CAL/DOL ternary diagrams showing the contrast between the relative proportions of sedimentary lithologies at the source (Siliciclastics/Limestones/Dolostones), and sand composition for coarse, medium and fine fractions of low order stream deposits from the Iberian Range. Data have been arbitrarily split into three groups as a function of the dolomite content at the source ((a) 85% to 100% Dol. (b) 45% to 85% Dol. (c) <35% Dol). Dots and hexagons indicate means and 95% confidence levels.

area is less (Fig. 7b and c). These diagrams also reflect the considerable ability of sandstones to produce sands causing the dilution of carbonate components. Thus, the occurrence of 16% of siliciclastic rocks at the source may produce a sand with 75% of non-carbonate grains (Fig. 7b). This fact is more noticeable if dolostone is the accompanying lithology at the source. However, the presence of limestones at the source reduces the over-representation of siliciclastics in the sands, mainly in the medium and coarse fractions where limestone grains concentrate (Fig. 7c).

In many cases, marls are a major lithological component at the source, constituting as much as 34% of surface area (Appendix B). However, there is no grain type in the stream sands clearly related to that source. Marls mainly produce very fine grain sized sediments (<62 μm) as a consequence of their lack of consistency and their fine grained texture. Therefore, their capacity to produce sandy deposits is very limited. However, it is assumed that marls do not have a purely fine grained texture but may contain a wide spectrum of non-carbonate or carbonate sand grains (i.e., fossils; Cavazza et al., 1993). The presence of these grains in the sands is not very significant if compared with contributions from other source rocks, and therefore marl supplies are unlikely to disturb the general source/sediment contrast.

Several petrographic indices (AN/(AN + AC), DOL/AC, Lmwp/AC, Dm/AC, Lgec/AC and Dr/AC) have been considered for more accurate analysis of the representativeness of diverse grain types when compared with their parent sources. Detailed data on the bedrock lithology can be used to calculate an equivalent ratio of occurrence of lithologic types at

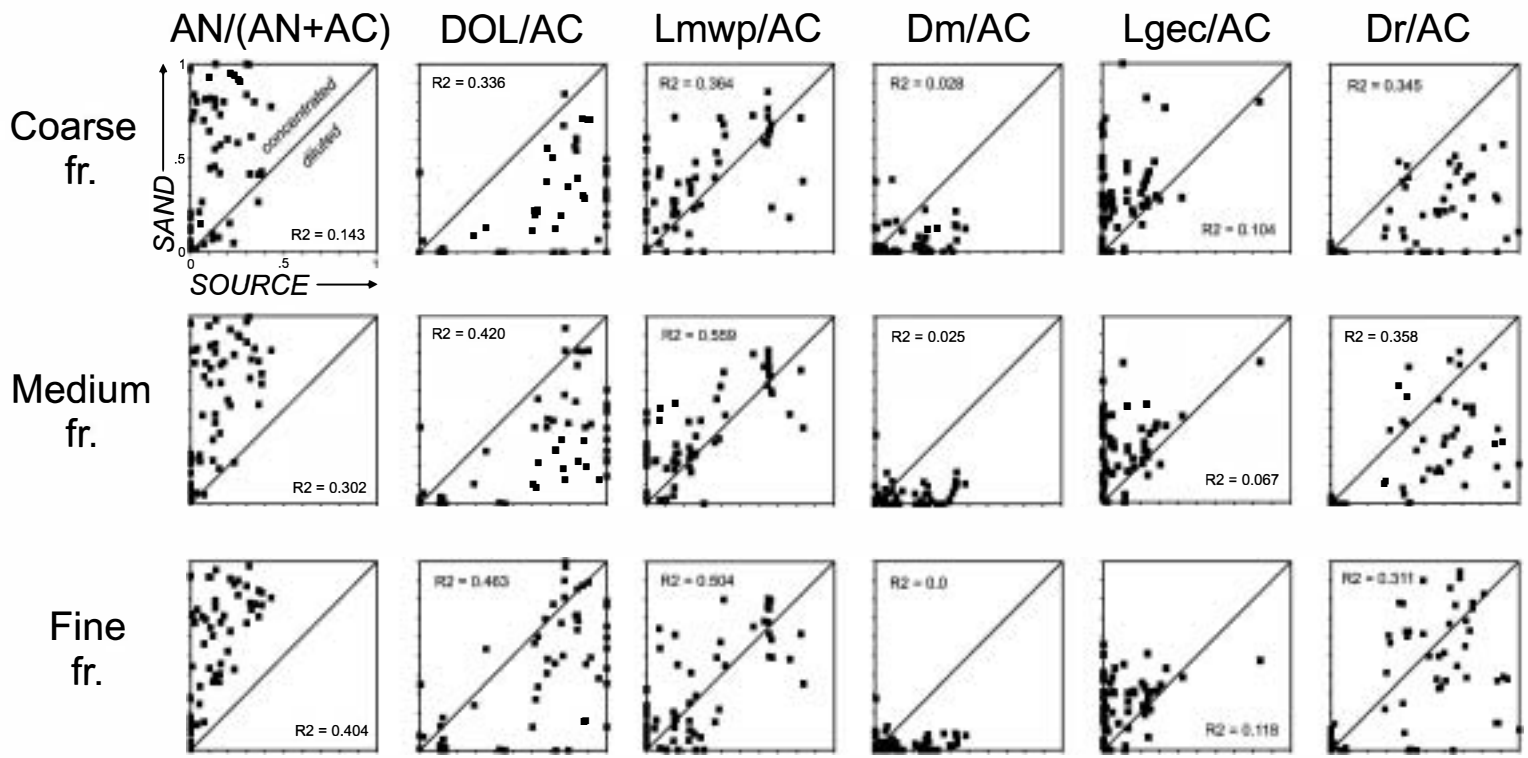

Fig. 8. Plots of several petrographic indices versus the corresponding indices of surface exposure of lithologies at the source for coarse, medium and fine fractions of low order stream deposits from the Iberian Range. For explanation of petrographic indices, see Table 1.

the sources (Fig. 8). This type of diagram appears to be very useful when sources are analyzed as sediment producers (Mack, 1981; Palomares and Arribas, 1993; Arribas et al., 2000). Siliciclastic sources are the most productive sedimentary source of sand in the three analyzed fractions appearing in the upper part of the diagrams (concentration zone). Dolomitic formations are the least productive carbonate sources (DOL/AC and Dm/AC, Fig. 8) plotted in the lower part of the diagrams (dilution zone). Micritic limestones (Lmwp) show the best fit with the sand composition, with $R^2 = 0.559$ in the medium size fraction. The behavior of sparitic textures as sand producers is controlled by their composition. Thus, sparitic limestones (Lgec) are concentrated and over-represented in the three sand fractions, whereas sparitic dolostones (Dr) are under-represented in coarse and medium sand fractions.

Slope data from Appendix B have been compared with medium-grained sand compositions to evaluate the influence of this physiographic variable on sand generation. Fig. 9 shows similar diagrams to those of Fig. 8, in which samples have been arbitrarily grouped in two categories as a function of slope values: (1)

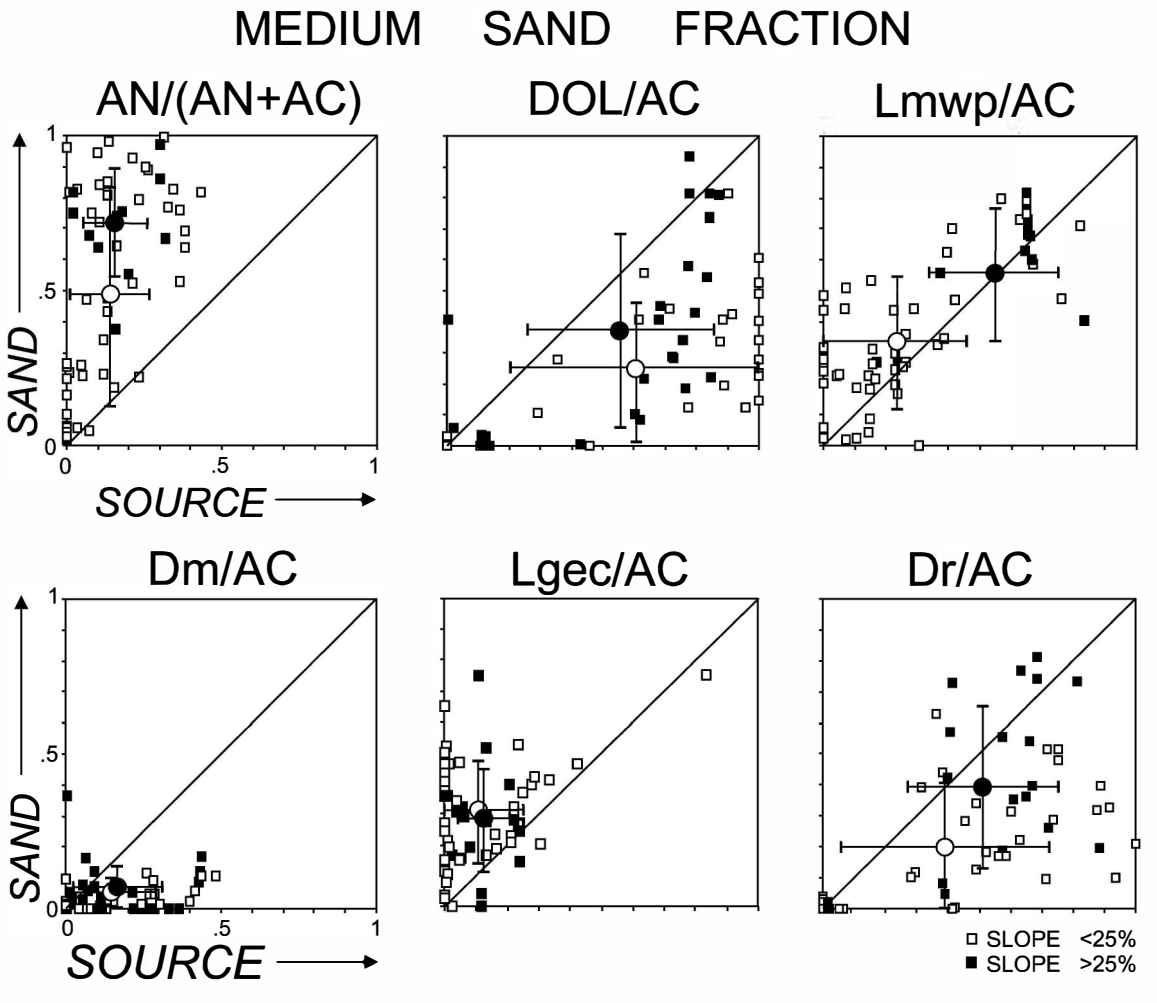

Fig. 9. Plots of several petrographic indices versus the corresponding indices of surface exposure of lithologies in the source area for the medium sand fraction of low order stream deposits from the Iberian Range. Samples are grouped as a function of slope (< 25% and >25%). Means and standard deviations of each group of samples are also shown.

Samples from sub-basins with slope of a given bedrock <25%, and (2) samples from sub-basins with slope of a given bedrock >25%. Generally the cluster (means) of samples related to steep slopes (>25%) has a sand composition enriched in the analyzed components, plotting in higher positions in the diagrams than the gentle slope cluster (<25%) (Fig. 9). This means that slope increase enhances the compositional signal of a given bedrock in the related sand. Slope influence on sand composition is only clearly manifested in siliciclastic bedrocks (AN/(AN+AC) diagram in Fig. 9) probably due to the propensity to granular disintegration of these rocks. However, a detailed statistical study is required to evaluate the role of this variable for each bedrock type. The narrow range of slope values (15 to 35%) and the limitations of bedrock occurrences obstruct this evaluation, which is far of the aim of this paper.

6. Discussion

6.1. The SGI of sedimentary sources

Sand generation indices (SGIs), as defined by Palomares and Arribas (1993), are difficult to calculate from the above results (Fig. 8) because the values are highly dispersed. However, a semi-quantitative approach may help gain a better understanding of the behavior of sedimentary sources as sand producers.

As proposed by Palomares and Arribas (1993), the SGI of a given bedrock type is a variable that reflects the relative sand-generating capability of that bedrock when compared to other bedrock types that are generating sand under the same topographic and climatic conditions. The SGI of a given bedrock type A of a dual source A+B ($SGI_{A(A+B)}$) is expressed in terms of the outcrop area of A (S_A) needed to produce a sand with equal amounts of grains from both A and B bedrocks. This variable is given by

$$SGI_{A(A+B)} = [S_A + S_B]/S_A \quad (1)$$

where $[S_A + S_B]$ is the total surface area of the source area (100%), and S_A and S_B are the outcrop areas of bedrock types A and B within the source area to produce the sand with average modal composition. Likewise, the SGI for bedrock type B in the pair is given by

$$SGI_{B(A+B)} = [S_A + S_B]/S_B \quad (2)$$

In our case, the pairs of sedimentary bedrocks considered are those represented in Fig. 8 (Siliciclastic (AN)+Carbonates (AC); Dolomite (DOL)+Limestone (CAL); Micritic limestones (Lmwp)+Rest of carbonates (AC-Lmwp); Dolomicrite (Dm)+Rest of carbonates (AC-Dm); Sparitic limestones (Lgec)+Rest of carbonates (AC-Lgec); Sparitic dolostones (Dr)+Rest of carbonates (AC-Dr)). Unequivocal composition of derived grain types (i.e., a Dm grain is considered as provided by dolomicrite rocks at the source) facilitates the calculation of the average modal composition between end-members of pairs. This average modal composition corresponds to the mid-point of *Y*-axis (0.5) of diagrams in Fig. 8. From this point, a range in of surface area for both end-members of each pair can be visually estimated by reading in the *X*-axis of diagrams in Fig. 8. For example, considering a source area constituted by siliciclastics+carbonates (AN/(AN+AC) in Fig. 8), the average modal composition of a medium grained sand is generated when siliciclastic rocks represent from 5 to 25% of total surface area of the drainage sub-basin. These values can be used to obtain an approximate SGI for siliciclastic and carbonate rocks from Eqs. (1) and (2).

Obtained SGI values are shown in Table 3 for medium grain size deposits and for the different pairs of bedrocks at the sources. Thus, in the case of sources constituted by carbonates and siliciclastic rocks the SGI of siliciclastic sources varies from 20 to 4, whereas the SGI of carbonates varies from 1.0 to 1.3. This means that siliciclastic formations are 3 to 20 times more efficient in producing medium sized sand than carbonates. Limestones (SGI from 5.5 to 3.3) have 3 to 4 times more capacity to generate medium sand than dolostones (SGI from 1.2 to 1.4) in sources constituted by carbonates exclusively. In addition, texture controls sand production from the different carbonate sources. Thus, sparitic limestone presents the highest SGI values (2.0–2.8), nearly 10 times greater than sparitic dolostones (SGI of 2.5–1.3) and nearly 20 times greater than dolomicritic

Table 3
SGI values from compound sedimentary source areas (medium grain size)

Compound sedimentary source	Surface area corresponding to average composition[a] (%)	SGI	SGI when increasing grain size
Siliciclastics + carbonates			
Siliciclastics	5–25	2.0–4	decreases
Carbonates	95–75	1.0–1.3	increases
Dolostones + limestones			
Limestones	18–30	5.5–3.3	increases
Dolostones	82–70	1.2–1.4	decreases
Carbonate lithofacies			
Micritic limestones (Lmwp)	35–45	2.8–2.2	increases
Rest of carbonates (AC-Lmwp)	65–55	1.5–1.8	decreases
Micritic dolostones (Dm)	(100)	(1)	(increases)
Rest of carbonates (AC-Dm)	(0)	(–)	(decreases)
Sparitic limestones (Lgec)	5–35	2.0–2.8	steady
Rest of carbonates (AC-Lgec)	95–65	1.0–1.5	steady
Sparitic dolostones (Dr)	40–75	2.5–1.3	decreases
Rest of carbonates (AC-Dr)	60–25	1.6–4	increases

[a] Visual estimation from diagrams in Fig. 8.

sources. On the other hand, there is little variation in SGI values when grain size varies. Generally, the SGI of siliciclastic and dolostone formations decreases when sand grain size increases. Variation in the SGI of the different textures when grain size increases is most evident in micritic limestones (increasing trend) and sparitic dolostones (decreasing trend) (Fig. 8 and Table 3).

6.2. The preservation of carbonate grains

Little information is available on the relative stability of the different carbonate grains in weathering environments. Exclusively, a general statement is widely assumed: climate plays a vital role in the preservation of carbonate rock fragments because of the high susceptibility of carbonate to dissolution under humid climate conditions (Potter, 1978, 1994; Blatt et al., 1980; Mack, 1981). Dolomite exhibits greater mineral stability than calcite as a function of size and distortion of CaO_6 and MgO_6 octahedra (Reeder, 1983). Thus, pure dolomite is less soluble than calcite (Bathurst, 1975; pp. 252–254). In addition, the texture of carbonates (microfacies) may control their solution rate. A smaller crystal size produces a larger reaction surface, enhancing solubility (Bathurst, 1975; p. 254; Chave and Schmalz, 1966; p. 1045). Therefore, dolospar grains are the most stable carbonate grains, and hence over-representation of this carbonate grain category may be expected in the sand. On the other hand, micritic limestones should be consistently under-represented in the sand, as their texture is less stable to chemical weathering. However, our results do not seem to bear out these assumptions. Upper Cretaceous dolomite formations exhibit important dedolomitization processes manifested by a wide spectrum of textures (Fernández Calvo, 1981). These textures are also visible in their sandy products as large calcite crystals embedding dolomite relicts. It is clear that dedolomitization appears as a decisive process in sparry calcite production, weighting the calcite side. Unfortunately, quantitative evaluation of this process is not feasible on the scale of this work. Dedolomitization works at any scale, from microscopic level to areas of thousands of meters, affecting cartographic units partial or even totally, with several grades of intensity (Fernández Calvo, 1981). Thus, cartographic expression of this process is not possible. However, it is expected that the origin of many calcite single crystals (Lc) found in sands will be related to dedolomitization processes at the sources. Fig. 10 shows that the content of (Lc + Dr) grains in coarse and medium sand fractions fits the Dr/AC surface distribution at the sources better, supporting the idea that many calcite

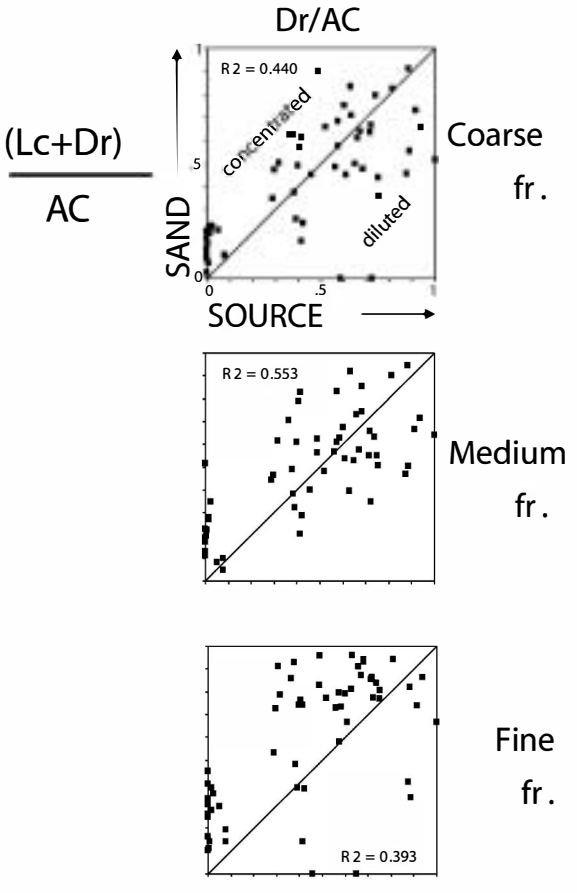

Fig. 10. Comparison of coarse-crystalline dolomite grains plus calcite single crystal grains in ancient carbonate grains ((Lc + Dr)/AC) versus coarse-crystalline dolomite in ancient carbonate rocks (Dr/AC) at the source for coarse, medium and fine sand fractions of low order stream deposits from the Iberian Range. For explanation of petrographic indices, see Table 1.

crystal grains are provided by dolomite terrains. On the other hand, it is difficult to explain the fact that dolomicrite grains are less well represented than micritic limestone grains. Dedolomitization processes have not been described in the dolomicritic formations, and thus the considerable under-representation of this texture cannot be explained by replacements occurring during diagenesis of these bedrocks. Several authors have pointed to the influence of the uptake of different nutrient elements during pedogenesis in the depletion of specific minerals (i.e., Moulton and Berner, 1998). Probably, processes favoring the capture of Mg^{2+} ion by plants during soil development are involved in the loss of dolomicrite in the regolith. However, we cannot confirm this fact, which in any case falls without the scope of this work.

7. Concluding remarks

Sedimenticlastic sands from head streams in the Iberian Range present a variable quartzolithic composition with variable amounts of penecontemporaneous carbonate clasts. Variations in composition are also observed when grain size varies. Penecontemporaneous carbonate grains are concentrated in the fine sand fraction, while micritic and sparitic limestone grains and micritic dolostone grains are concentrated in the coarse sand fraction. Recycled K-feldspar from arkosic bedrock tends to be concentrated in the fine sand fraction.

Contrasts between the composition of modern sedimenticlastic sands in head streams and the different proportions of the specific sedimentary rocks constituting the source terrains provides information about the behavior of these sources as sand producers.

Ternary (AN-CAL-DOL) and binary diagrams comparing sand petrographic indices with source occurrence indices (AN/(AN + AC), DOL/AC, Lmwp/AC, Dm/AC, Lgec/AC and Dr/AC) have proved very useful in evaluating the sand production of each bedrock lithology.

Siliciclastic formations (sandstones) appear to be the most productive sedimentary source of sand, their occurrence at the source always over-represented in the sediment. Thus, 5% to 25% of siliciclastic formations at the source is enough to produce 50% of siliciclastics in the sand when these formations are accompanied by carbonate bedrocks. This indicates that the productivity of siliciclastic formations is 3 to 20 times greater than that of carbonates (SGI of siliciclastic formations: 4–20).

In sources constituted solely by carbonates, sand production varies according to the rock composition and texture. Limestones exhibit 3 to 4 times more capacity to generate sands than dolostones, while sparitic limestones present the highest SGI values (2.8 to 20). However, this over-representation of sparitic limestones in a direct reading from sand composition may be a misleading interpretation. Sparitic calcite grains can be derived from sources other than sparitic limestones, such as calcite cement in

sandstones (Cavazza et al., 1993), calcite veins, and dedolomitic formations. As evidenced in this study, calciticed dolomitic bedrocks are a consistent source of sparitic calcite grains.

Micritic limestone is the carbonate component in the sediment that best represents the proportion of the bedrock at the source when this is constituted solely by carbonate rocks. On the other hand, dolomicritic grains are the carbonate components that exhibit the most dilution, under-representing this lithology at the source.

It should be noted that our results refer to the behavior of sedimentary bedrocks during the first stage of sand generation, with negligible sediment transport effects. However, these data may help in deciphering the paleogeography and composition of sources of ancient sedimenticlastic deposits.

Future research needs to focus on larger-scale sampling to evaluate modifications of sand composition with prolonged transport.

Acknowledgements

This work was funded by a DGICYT project PB93-0178 (Grants to J. Arribas). We are grateful to K.A.W. Crook, A.C. Morton and A. Di Giulio for reviews and helpful discussions on an early version of the manuscript. Thanks to Daniel Arribas for his help in mathematical treatment of data.

Appendix A. Sand composition data set

Coarse fraction (1 0.5 mm)

	CU-13	CU-14	CU-15	CU-16	CU-17	CU-18	CU-19	CU-21	CU-22	CU-23	CU-42	MA-11	MA-12	MA-13	MA-14	MA-15	MA-31	MA-32[a]	MA-33	MA-34
Qs	7	54	128	239	117	24	225	182	150	113	1	56	179	152	167	176	33		13	3
Qp	3	17	74	108	45	11	103	89	80	43	0	20	62	69	89	70	6		1	1
Qi	0	0	1	0	0	2	0	1	0	0	0	0	1	1	4	0	1		1	0
Qr	0	3	10	11	1	0	2	3	1	2	0	0	0	3	0	4	0		0	0
Ks	0	3	24	38	2	4	18	18	14	10	1	2	0	6	0	11	0		0	0
Kr	0	1	4	2	0	1	1	2	1	1	0	0	1	2	3	0	0		0	0
Mf	0	0	0	1	0	0	1	0	1	0	0	0	0	0	0	1	0		0	0
Ch	0	0	0	0	0	0	0	0	0	0	0	0	0	0	0	2	0		0	0
Mc	0	0	0	0	0	0	0	0	0	0	0	0	0	0	0	0	0		0	0
Ot	0	0	1	0	2	1	4	3	4	6	4	0	5	2	5	1	5		1	0
Sc	0	3	15	1	5	0	0	1	0	4	0	0	1	3	3	1	0		0	0
Sf	0	0	1	0	1	1	2	0	1	1	0	0	1	0	1	1	0		0	0
Sm	0	0	0	0	1	0	0	0	0	0	0	0	0	0	0	1	0		0	0
Lm	0	11	2	0	0	0	0	4	25	67	38	65	14	20	8	17	33		6	22
Lmb	0	1	0	0	0	0	0	2	11	15	25	5	10	3	5	4	18		4	3
Lmr	1	0	0	0	1	0	0	3	1	11	36	21	7	4	1	1	15		5	15
Lg	0	0	0	0	0	0	0	3	2	6	26	0	1	2	1	1	2		0	1
Le	1	1	0	0	6	2	0	4	3	17	85	18	0	7	3	10	91		18	39
Lc	0	0	2	1	4	1		4	12	14	25	5	4	3	5	11	54		5	8
Fe	0	0	0	0	0	0	0	0	0	0	1	0	2	2	2		2		0	1
Ls	0	5	4	0	4	2	0	0	3	10	15	0	7	3	2	3	4		1	2
Dm	0	0	1	0	0	0	0	0	0	0	0	3	5	13	12	13	0		3	1
De	0	1	0	0	0	0	1	3	4	0	2	0	1	15	6	13	0		3	0
Dc	0	0	1	0	0	0	0	0	0	0	0	0	0	21	10	12	1		0	0
Dd	0	0	2	0	1	7	1		1	0	28	4	6	9	3	10	77		16	17
Ds	0	0	5	0	0	0	0	0	0	0	2	1	1	0	0	1	0		1	0
Bio	0	0	0	0	0	1		1	1	3	1	1	1	0	0	0	0		2	2
In	295	49	7	5	2	83	1	0	1	7	2	32	5	5	1	2	2		22	56
XQm	28	110	24	1	51	63	7	1	3	4	0	19	5	7	0	14	1		67	2
XQp	18	73	14	0	29	37	2	1	0	3	0	4	3	2	7	3	0		35	2
XQi	0	0	0	0	1	0	0	0	0	0	0	0	0	0	0	1	0		0	0
XQr	1	2	2	0	0	0	0	0	0	0	0	0	1	0	0	0	0		1	0
XKs	1	10	5	1	4	2	0	0	0	0	0	0	0	0	1	0	0		0	0
XKr	1	2	0	0	1	0	0	0	0	0	0	0	0	0	0	0	0		0	0
XMf	0	0	0	0	0	0	0	0	0	0	0	0	0	0	0	0	0		1	0
XCh	0	0	0	0	0	0	0	0	0	0	0	0	0	0	0	0	0		4	0
XMc	0	0	0	0	0	0	0	0	0	0	0	0	0	0	0	0	0		0	0
XOt	1	3	1		3	2	0	0	0	0	0	0	0	0	0	0	0		1	0
XSc	0	0	0	0	0	0	0	0	0	0	0	0	0	0	0	0	0		0	0
XSf	0	0	0	0	1	0	0	0	0	0	0	0	0	0	0	0	0		1	0
XSm	0	0	0	0	0	0	0	0	0	0	0	0	0	0	0	0	0		0	0
XLm	0	0	0	0	1	3	0	0	1	0	0	1	0	0	1	0	0		5	1
XLm	0	0	0	0	0	0	0	0	0	0	0	0	0	0	0	0	0		2	0
XLmr	0	0	0	0	0	1	0	0	0	0	0	0	0	0	0	0	0		2	6
XLg	0	0	0	0	0	0	0	0	0	0	0	0	0	0	0	0	0		0	0
XLe	1	6	0	0	2	11	0	0	1	0	1	0	0	1	0	0	0		19	12
XLc	0	3	0	0	3	1	0	0	0	0	0	0	2	0	0	0	0		15	4
XFe	0	0	0	0	0	0	0	0	0	0	0	0	0	0	0	1	0		1	0
XLs	1	0	0	0	0	0	0	0	0	0	0	0	0	0	0	0	0		2	2
XDm	0	2	0	0	0	1	0	0	0	0	0	1	0	0	0	1	0		3	1
XDe	0	0	0	0	1	1	0	0	0	0	0	1	0	0	0	2	0		11	1
XDc	0	0	0	0	0	0	0	0	0	0	0	1	0	0	0	1	0		1	2
XDd	0	0	0	0	2	3	0	0	0	0	0	4	0	0	0	0	0		28	7
XDs	0	0	0	0	0	0	0	0	0	0	0	0	0	0	0	0	0		2	1
XBio	0	0	0	0	0	1	0	0	0	0	0	0	0	0	0	0	0		0	0
XIn	14	1	0	0	0	4	0	1	0	0	0	3	0	0	0	0	0		2	6
En	8	21	3	0	5	10	0	0	0	0	0	5	0	0	1	3	1		12	5
Total	381	382	331	408	294	280	368	326	321	337	301	281	348	355	363	400	362		317	225

[a] Non-available sand from this fraction.

MA-35	MA-42	MA-43	MA-44	MA-45	MA-46S	CÑ-21	CÑ-21S	FU-11	FU-12	FU-31	FU-41	FU-43[a]	FU-45	FU-46	FU-410	FU-411	FU-411S	TR-31
5	71	124	26	8	12	17	81	234	11	36	34		22	24	95	136	235	23
4	29	67	17	3	5	4	44	122	1	10	21		16	19	44	115	143	17
0	0	0	3	0	1	0	0	1	1	0	1		0	16	2	1	0	0
0	2	8	0	1	0	0	2	11	0	0	4		1	0	3	7	13	0
0	1	9	0	0	1	2	6	23	0	0	0		2	3	6	8	8	0
0	2	3	0	0	0	0	0	3	0	0	0		0	1	1	0	1	0
0	0	0	1	2	0	0	0	1	0	0	0		1	5	3	1	2	0
0	1	0	0	0	0	0	0	0	0	0	0		0	2	0	1	0	0
0	0	0	0	0	0	0	0	0	0	0	0		0	0	0	0	0	0
1	45	3	0	3	2	0	0	0	2	1	1		3	2	3	1	0	3
0	0	0	0	1	0	1	6	0	0	0	0		0	1	0	0	0	0
0	0	0	0	0	0	0	1	0	0	0	0		0	0	1	0	0	0
0	0	0	0	0	0	0	0	0	0	0	0		0	0	0	0	3	0
24	18	21	84	18	19	2	11	0	5	15	5		5	9	6	6	0	18
4	3	1	10	183	199	0	5	0	0	5	0		7	4	8	1	0	4
22	2	0	41	1	1	0	3	0	2	4	0		0	0	0	0	0	15
1	1	1	10	3	1	0	1	1	0	0	1		1	2	2	0	0	14
33	5	1	72	4	13	0	4	6	16	6	2		3	20		0	0	36
24	4	6	15	8	11	1	9	4	66	5	0		5	36	3	1	0	39
0	1	1	0	7	8	0	1	0	0	1	1		0	2	2	1	0	0
6	1	0	10	1	1	0	4	1	0	1	0		1	2	0	1	0	3
18	0	12	21	3	14	0	1	0	47	3	9		11	63	9	20	0	0
19	1	18	15	69	59	1	4	0	53	1	8		3	70	13	18	0	1
2	6	18	0	0	2	1	1	0	34	2	4		3	49	8	3	1	1
42	1	6	57	80	44	0	3	0	82	2	2		3	10	3	1	0	10
2	0	0	2	1	0	0	0	0	0	0	0		0	0	0	0	0	0
0	5	0	0	0	0	9	1	0	0	1	2		2	2	0	1	0	2
6	3	1	4	7	4	301	4	0	7	6	29		17	38	14	49	0	153
3	44	8	0	0	0	23	90	0	0	56	107		79	4	70	6	0	2
0	17	7	1	0	0	9	56	0	0	29	55		62	4	45	5	0	2
1	0	0	0	0	0	0	0	0	0	0	0		0	1	2	0	0	0
0	1	0	0	0	0	1	8	0	0	0	2		0	0	1	0	0	0
0	0	0	0	0	0	3	11	0	0	4	10		8	0	5	0	0	1
0	0	0	0	0	0	1	2	0	0	0	1		0	0	2	0	0	0
0	0	0	0	0	0	0	0	0	0	0	0		0	0	0	0	0	0
0	1	0	0	0	0	0	0	0	0	0	0		1	0	0	0	0	0
0	0	0	0	0	0	0	0	0	0	0	0		0	0	0	0	0	0
0	13	0	0	0	0	0	1	0	0	5	2		4	0	2	0	0	0
0	0	0	0	0	0	0	2	0	0	0	0		3	0	0	0	0	0
0	0	0	0	0	0	0	0	0	0	0	0		0	0	1	0	0	0
0	0	0	0	0	0	0	0	0	0	0	0		0	0	0	0	0	0
2	1	0	3	0	1	2	4	0	0	4	15		18	2	4	0	0	5
0	0	0	0	0	0	0	4	0	0	4	7		20	0	2	0	0	2
0	0	1	1	0	0	0	2	0	0	4	2		4	0	0	0	0	10
0	0	0	0	0	0	0	4	0	0	0	0		3	3	1	0	0	2
11	0	0	0	0	0	2	5	0	0	3	12		11	2	2	0	0	21
6	5	7	1	0	0	3	14	0	0	7	13		23	13	5	0	0	25
0	1	0	0	0	0	1	1	0	0	2	3		12	2	4	1	0	1
1	0	0	0	0	0	0	0	0	0	0	1		0	0	1	0	0	2
13	0	0	0	0	0	0	1	0	0	11	7		7	7	7	0	0	0
7	0	0	0	0	0	0	1	0	1	6	14		10	7	18	0	0	0
2	3	4	0	1	0	0	1	0	0	5	20		8	10	1	2	0	0
22	0	0	0	1	0	1	7	0	0	4	6		10	0	7	0	0	2
1	0	0	0	0	0	0	0	0	0	0	0		1	0	0	0	0	0
0	0	2	0	0	0	0	0	0	0	0	0		0	0	0	0	0	0
0	0	0	0	0	1	13	0	0	0	0	0		0	1	2	4	0	19
4	3	2	0	0	0	7	8	0	0	4	9		8	3	6	3	0	6
286	291	331	394	405	399	405	416	407	328	247	410		408	439	415	393	406	439

(continued on next page)

Appendix A (*continued*)

	TR-41	TR-42	TR-43	TR-44S	TR-45S	TE-11	TE-12	TE-12S	TE-13	TE-14	TE-15	TE-16	TE-31	TE-32	TE-33	TE-34	TE-35	TE-35S	TE-36	TE-37	TE-37S
Qs	1	1	111	30	71	1	1	5	1	13	185	140	148	2	33	36	82	54	82	94	81
Qp	1	2	39	10	43	0	1	4	0	4	71	55	84	3	10	7	24	33	38	39	49
Qi	0	0	0	0	0	0	0	0	0	0	0	0	1	0	1	0	0	0	0	0	0
Qr	0	0	2	1	1	0	0	0	0	0	0	3	4	0	0	0	4	1	0	1	3
Ks	0	0	8	2	5	0	0	0	0	0	24	14	15	0	1	1	10	6	10	8	9
Kr	0	0	1	0	0	0	0	0	0	0	1	2	2	0	0	0	0	0	1	0	0
Mf	3	7	2	20	9	0	0	0	0	6	0	1	0	1	0	0	2	1	0	2	0
Ch	0	0	3	0	1	0	3	2	1	0	0	0	0	0	0	0	0	0	1	3	3
Mc	0	0	0	0	0	0	0	0	0	1	0	0	0	0	0	0	0	0	0	0	0
Ot	1	0	12	11	11	5	4	8	2	8	9	3	3	1	8	16	12	9	5	9	4
Sc	1	0	43	25	26	14	10	18	2	29	6	7	8	0	4	4	25	8	27	12	18
Sf	0	0	1	1	1	5	0	0	0	0	0	0	1	0	0	0	1	0	0	0	0
Sm	0	0	3	9	5	0	0	0	0	2	0	0	0	0	0	2	3	1	1	0	2
Lm	77	39	14	27	29	189	158	151	78	86	30	54	23	14	42	35	122	156	114	113	94
Lmb	75	33	7	21	6	28	25	28	21	63	11	18	11	26	83	37	9	12	15	15	20
Lmr	3	0	9	2	8	37	19	6	19	5	1	8	3	5	12	8	7	4	11	10	10
Lg	14	27	91	217	124	58	16	34	37	53	26	29	9	9	34	7	31	26	19	34	29
Le	8	11	20	2	10	23	8	10	21	12	1	4	4	35	18	17	6	13	17	12	4
Lc	13	1	12	5	6	15	9	16	4	16	3	13	4	27	19	8	15	16	27	29	38
Fe	53	32	3	11	9	10	5	6	1	7	1	3	4	1	13	4	3	8	1	3	6
Ls	2	1	16	13	24	52	24	104	40	106	18	26	22	4	19	27	38	71	32	27	27
Dm	7	72	0	0	0	0	0	0	0	0	0	0	0	51	0	1	0	0	1	0	2
De	0	4	0	0	0	0	0	0	0	0	0	0	0	12	2	1	0	0	0	0	0
Dc	0	0	0	0	0	0	0	0	0	0	0	0	0	1	0	0	0	0	0	0	0
Dd	6	6	0	0	0	0	0	0	0	1	0	0	0	208	87	45	1	0	2	0	2
Ds	0	0	0	0	0	0	0	0	0	0	0	0	0	5	4	1	0	0	0	2	1
Bio	3	0	0	0	0	0	0	1	1	0	0	0	0	0	0	0	0	0	0	0	0
In	43	0	10	1	0	11	13	7	57	3	1	0	0	0	2	13	6	1	3	2	3
XQm	1	0	7	0	1	0	0	0	5	0	5	16	32	0	3	8	1	0	5	1	3
XQp	1	0	6	0	0	0	0	0	1	0	5	8	19	0	2	6	0	0	1	1	1
XQi	0	0	0	0	0	0	0	0	0	0	0	0	0	0	0	0	0	0	0	0	0
XQr	0	0	0	0	0	0	0	0	0	0	0	0	1	0	0	0	0	0	0	0	0
XKs	0	0	0	0	0	0	0	1	0	0	4	0	10	0	0	1	0	0	1	0	0
XKr	0	0	0	0	0	0	0	0	0	0	0	0	0	0	0	0	0	0	1	0	0
XMf	0	0	0	0	0	0	0	0	0	0	0	0	0	0	0	0	0	0	0	0	0
XCh	0	0	0	0	0	0	0	1	0	0	0	0	0	0	0	0	0	0	0	0	0
XMc	0	0	0	0	0	0	0	0	0	0	0	0	0	0	0	0	0	0	0	0	0
XOt	5	0	0	0	0	0	1	0	10	0	0	0	0	0	1	1	0	0	0	0	0
XSc	0	0	2	0	0	0	2	0	6	0	0	0	0	0	0	0	0	0	0	0	0
XSf	0	0	0	0	0	0	1	0	0	0	0	0	0	0	0	0	0	0	0	0	0
XSm	0	0	0	0	0	0	0	0	0	0	0	0	0	0	0	0	0	0	0	0	0
XLm	10	0	2	0	0	2	77	2	25	0	0	0	1	0	0	11	0	0	0	0	0
XLmb	11	0	0	0	0	0	5	1	7	0	0	0	0	0	0	5	0	0	0	0	0
XLmr	1	0	0	0	0	0	6	0	12	0	0	0	0	0	0	7	0	0	0	0	0
XLg	5	0	0	0	0	1	1	1	18	0	0	0	0	0	1	1	0	0	0	0	0
XLe	8	0	0	0	0	0	6	0	19	0	1	0	0	0	3	25	1		0	1	1
XLc	8	0	0	0	0	0	10	0	13	1	0	3	1	0	10	21	0	0	1	0	0
XFe	38	0	0	0	0	0	1	0	2	0	0	0	1	0	0	15	0	0	0	0	0
XLs	0	0	0	0	0	0	2	3	13	0	0	0	0	0	0	2	0	0	0	0	0
XDm	2	0	0	0	0	0	0	0	0	0	0	0	0	0	0	0	0	0	0	0	0
XDe	0	0	0	0	0	0	0	0	1	0	0	0	0	0	1	0	0	0	0	0	0
XDc	0	0	0	0	0	0	0	0	0	0	0	0	0	0	0	0	0	0	0	0	0
XDd	0	0	0	0	0	0	0	0	0	0	0	0	0	0	1	27	0	0	0	0	0
XDs	0	0	0	0	0	0	0	0	0	0	0	0	0	0	0	0	0	0	0	0	0
XBio	0	0	0	0	0	0	0	0	0	0	0	0	0	0	0	0	0	0	0	0	0
XIn	0	0	0	0	0	0	0	0	3	0	0	0	0	0	0	0	0	0	0	0	0
En	2	0	3	0	0	0	6	0	10	0	0	0	0	0	0	2	0	0	0	0	0
Total	406	236	424	408	390	447	418	411	430	416	405	407	411	405	422	407	403	414	414	418	410

Appendix A (*continued*)

Medium fraction (0.5 0.25 mm)

	CU-13	CU-14	CU-15	CU-16	CU-17	CU-18	CU-19	CU-21	CU-22	CU-23	CU-42	MA-11	MA-12	MA-13	MA-14	MA-15	MA-31	MA-32	MA-33
Qs	9	149	222	262	187	121	264	255	209	163	13	78	222	241	229	254	46	65	64
Qp	4	62	56	60	59	38	92	73	63	46	1	16	44	65	51	51	12	12	9
Qi	0	0	0	2	0	0	1	1	0	2	3	0	2	0	1	1	2	4	0
Qr	0	1	4	3	4	0	2	4	4	1	1	0	2	0	0	0	0	0	1
Ks	1	19	47	69	34	9	16	41	44	27	0	7	24	10	14	9	7	6	8
Kr	0	0	1	3	1	1	3	4	5	0	0	0	1	0	1	0	0	0	1
Mf	0	0	1	0	2	1	1	3	3	1	2	0	1	2	2	0	1	0	1
Ch	0	1	1	1	0	2	0	0	0	0	0	0	0	0	0	0	0	0	0
Mc	0	0	0	0	0	0	0	0	0	0	0	0	0	0	0	0	0	0	0
Ot	0	5	5	2	12	2	10	6	11	19	5	2	7	4	5	1	0	0	2
Sc	0	0	1	0	2	0	1	4	1	1	1	0	0	0	0	0	0	0	0
Sf	0	0	0	0	0	0	1	0	0	1	0	0	1	0	1	1	0	0	0
Sm	0	0	0	0	0	0	1	0	0	0	0	0	0	0	1	0	0	0	0
Lm	0	7	3	1	2	15	0	1	13	27	31	78	42	2	13	3	74	47	33
Lmb	0	3	5	2	3	8	0	2	13	29	30	3	4	0	8	3	8	13	6
Lmr	0	0	0	0	0	0	0	3	5	11	37	25	6	1	5	0	10	33	2
Lg	0	0	1	0	0	0	0	1	0	18	25	0	5	0	1	0	6	2	0
Le	4	1	0	2	6	12	0	4	8	26	78	44	25	5	13	4	57	60	26
Lc	1	3	1	1	4	4	0	2	13	10	81	2	1	10	5	3	61	76	34
Fe	0	4	0	0	0	1	0	1	4	11	4	2	5	1	2	3	12	14	3
Ls	1	1	0	0	3	5	0	3	2	7	11	1	2	0	1	0	4	6	3
Dm	0	0	0	0	0	0	0	3	0	0	9	9	0	12	12	6	8	17	20
De	0	3	3	1	8	4	0	1	4	0	10	1	5	17	10	24	33	35	23
Dc	1	1	5	0	1	0	0	1	1	0	1	5	2	23	27	25	24	0	11
Dd	0	1	0	0	2	6	2	0	0	0	64	2	1	0	5	0	46	16	0
Ds	0	0	2	0	2	0	0	0	0	0	0	0	0	0	0	0	0	0	0
Bio	15	7	0	2	3	11	0	0	0	1	0	0	0	0	0	0	0	0	0
In	475	59	2	4	20	99	0	0	2	3	1	24	5	5	2	3	1	5	69
XQm	43	63	23	0	37	48	2	1	1	1	0	0	1	0	1	1	0	0	37
XQp	14	31	8	0	11	17	0	1	0	0	0	1	0	0	0	1	0	0	16
XQi	0	0	0	0	0	0	0	0	0	0	0	0	0	0	0	0	0	0	0
XQr	0	0	0	0	1	3	0	0	0	0	0	0	0	0	0	0	0	0	0
XKs	6	6	4	0	5	2	0	0	0	1	0	0	1	0	0	0	0	0	0
XKr	0	0	0	0	1		0	0	0	0	0	0	0	0	0	0	0	0	0
XMf	0	0	0	0	0	0	0	0	0	0	0	0	0	0	0	0	0	0	0
XCh	0	0	0	0	0	0	0	0	0	0	0	0	0	0	0	0	0	0	0
XMc	0	0	0	0	0	0	0	0	0	0	0	0	0	0	0	0	0	0	0
XOt	0	0	0	0	1	4	2	0	0	0	0	0	0	0	1	0	0	0	0
XSc	0	0	0	0	0	0	0	0	0	0	0	0	0	0	0	0	0	0	0
XSf	0	1	0	0	1	0	0	0	0	0	0	0	0	0	0	0	0	0	0
XSm	0	0	0	0	0	0	0	0	0	0	0	0	0	0	0	0	0	0	0
XLm	4	3	0	0	2	3	0	0	0	1	0	0	0	0	0	0	0	0	1
XLmb	0	0	0	0	0	1	0	0	0	0	0	0	0	0	0	0	0	0	0
XLmr	1	0	0	0	0	1	0	0	0	0	0	0	0	0	0	0	0	0	0
XLg	0	1	0	0	0	0	0	0	0	0	0	0	0	0	0	0	0	0	0
XLe	3	8	0	0	3	19	0	0	0	2	0	0	0	0	0	0	0	0	1
XLc	1	0	0	0	3	7	0	0	0	3	0	0	0	0	0	0	0	0	2
XFe	2	1	0	0	0	0	0	0	0	0	0	0	0	0	0	0	0	0	0
XLs	0	0	0	0	0	0	0	0	0	0	0	0	0	0	0	0	0	0	0
XDm	0	0	0	0	0	0	0	0	0	0	0	0	0	0	0	0	0	0	0
XDe	1	2	0	0	1	2	0	0	0	0	0	0	0	0	0	1	0	0	5
XDc	1	2	0	0	0	6	0	0	0	1	0	0	0	0	0	1	0	0	12
XDd	0	1	0	0	0	2	0	0	0	0	0	0	0	0	0	0	0	0	0
XDs	0	0	0	0	1	0	0	0	0	0	0	0	0	0	0	0	0	0	0
XBio	0	0	0	0	0	0	0	0	0	0	0	0	0	0	0	0	0	0	0
XIn	27	8	0	0	1	2	0	0	0	0	0	0	0	0	1	0	0	0	0
En	12	6	1	0	3	20	0	0	0	0	0	0	0	0	0	1	0	0	10
Total	626	460	415	415	426	476	400	415	415	415	410	300	415	398	412	400	412	411	400

(continued on next page)

Appendix A *(continued)*

	MA-34	MA-35	MA-42	MA-43	MA-44	MA-45	MA-46S	CÑ-21	CÑ-21S	FU-11	FU-12	FU-31	FU-41	FU-43	FU-45	FU-46	FU-410	FU-411	FU-411S	TR-31
Qs	11	10	134	171	46	5	5	21	160	273	10	96	82	32	50	60	198	230	246	33
Qp	2	2	38	69	10	2	0	6	66	67	2	30	31	3	28	14	45	73	102	14
Qi	0	0	0	0	4	0	0	0	0	3	1	0	0	0	0	6	0	0	0	0
Qr	0	0	2	4	0	0	0	0	1	6	0	0	2	1	1	0	0	0	1	0
Ks	0	0	13	12	1	1	0	4	25	40	5	4	7	4	0	1	21	5	32	7
Kr	0	0	0	1	0	0	0	0	0	1	0	0	2	0	0	0	0	0	0	0
Mf	2	0	25	4	3	0	1	1	0	2	0	0		0	0	0	2	0	6	0
Ch	0	0	1	2	0	0	0	0	0	1	0	0	0	0	0	0	1	0	0	0
Mc	0	0	0	0	0	0	0	0	0	0	0	0	0	0	0	0	0	0	0	0
Ot	0	2	39	3	0	0	1	0	4	0	6	2	3	5	5	18	2	3	2	2
Sc	0	1	0	0	1	0	0	0	1	0	0	0	1	0	1	0	0	0	0	1
Sf	0	0	0	0	0	0	0	0	2	0	0	0	0	0	1	0	0	0	0	0
Sm	0	0	0	0	0	0	0	0		0	0	0	0	0	1	0	0	0	1	0
Lm	21	69	15	22	56	25	12	1	15	0	8	13	18	9	21	3	14	1	2	18
Lmb	1	2	6	1	1	143	175	0	2	0	0	14	5	13	4	1	1	0	0	0
Lmr	7	19	6	0	43	1	1	0	0	1	1	5	0	1	4	0	5	0	0	14
Lg	0	0	1	1	1	1	0	0	1	0	0	1	0	4	1	1	1	0	0	1
Le	34	30	12	5	82	5	4	0	13	7	16	21	17	11	17	18	5	0	0	39
Lc	31	23	6	4	42	8	6	2	14	4	47	9	1	7	6	27	11	2	0	51
Fe	5	4	7	1	6	15	11	0	4	0	2	0	1	15	5	0	6	1	0	11
Ls	0	0	1	0	8	0	0	0	2	0	0	4	6	1	16	0	1	1	0	2
Dm	7	30	1	13	33	5	5	0	2	0	29	9	6	5	9	14	1	6	1	1
De	5	76	5	25	31	158	143	0	1	1	57	12	16	6	26	52	20	4	2	6
Dc	1	41	24	52	10	6	19	4	4	2	183	19	18	24	7	168	28	35	6	6
Dd	0	27	0	2	13	35	24	0	4	0	39	6	0	0	5	5	0	1	0	1
Ds	0	1	0	0	0	0	0	0	0	0	1	0	0	0	0	0	0	0	0	0
Bio	0	0	0	0	0	0	0	0	0	0	0	2	11	7	9	1	0	0	0	0
In	210	12	20	5	7	2	4	353	29	0	1	8	39	101	48	20	36	34	0	284
XQm	2	1	15	1	0	0	0	6	27	0	0	51	60	14	41	0	0	0	0	0
XQp	0	0	5	0	0	0	0	0	7	0	0	26	18	7	14	1	0	0	0	0
XQi	0	1	0	0	0	0	0	0	0	0	0	0	0	0	0	0	0	0	0	0
XQr	0	0	0	0	0	0	0	0	0	0	0	0	0	0	1	0	0	0	0	0
XKs	0	0	0	0	0	0	0	2	2	0	0	4	9	4	2	0	0	0	0	0
XKr	0	0	0	0	0	0	0	0	0	0	0	0	0	0	0	0	0	0	0	0
XMf	0	0	1	0	0	0	0	0	0	0	0	0	3	1	0	0	0	0	0	0
XCh	0	0	0	0	0	0	0	0	0	0	0	0	0	0	0	0	0	0	0	0
XMc	0	0	0	0	0	0	0	0	0	0	0	0	0	0	0	0	0	0	0	0
XOt	0	0	2	0	0	0	0	0	0	0	0	2	5	4	3	0	0	0	0	0
XSc	0	0	0	0	0	0	0	0	0	0	0	0	1	0	0	0	0	0	0	0
XSf	0	0	0	0	0	0	0	0	0	0	0	1	0	0	0	0	0	0	0	0
XSm	0	0	0	0	0	0	0	0	0	0	0	0	0	0	0	0	0	0	0	0
XLm	0	0	0	0	0	0	0	0	0	0	0	4	3	24	1	0	0	0	0	1
XLmb	0	0	0	0	0	0	0	0	0	0	0	8	2	4	5	0	0	0	0	0
XLmr	0	0	1	0	0	0	0	0	0	0	0	0	1	0	0	0	0	0	0	0
XLg	0	0	0	0	0	0	0	0	0	0	0	6	0	3	1	0	0	0	0	0
XLe	5	1	1	0	0	0	0	0	1	0	0	8	10	53	8	0	0	0	0	2
XLc	24	2	0	0	2	0	0	0	4	0	0	6	3	20	9	1	0	0	0	1
XFe	1	0	1	0	0	0	0	0	0	0	0	5	5	17	1	0	0	0	0	0
XLs	0	0	0	0	0	0	0	0	0	0	0	0	0	0	0	0	0	0	0	0
XDm	0	4	0	0	0	0	0	0	0	0	0	0	0	0	0	0	0	0	0	0
XDe	1	21	0	0	0	0	0	0	0	0	0	9	6	5	6	1	0	0	0	0
XDc	5	23	5	0	0	0	0	0	1	0	0	5	5	19	1	2	0	0	0	0
XDd	0	2	0	0	0	0	0	0	0	0	0	5	0	1	1	0	0	0	0	0
XDs	0	2	0	0	0	0	0	0	0	0	0	0	0	0	0	0	0	0	0	0
XBio	0	0	0	0	0	0	0	0	0	0	0	0	0	0	0	0	0	0	0	0
XIn	18	1	13	0	0	0	0	0	0	0	0	1	2	9	2	0	0	0	0	0
En	5	1	4	0	0	0	0	0	5	0	0	14	6	31	7	1	0	0	0	0
Total	400	412	400	400	400	413	413	400	399	410	412	414	409	465	376	421	400	400	401	501

TR-41	TR-42	TR-43	TR-44S	TR-45S	TE-11	TE-12	TE-12S	TE-13	TE-14	TE-15	TE-16	TE-31	TE-32	TE-33	TE-34	TE-35	TE-35S	TE-36	TE-37	TE-37S
2	7	241	64	228	32	21	38	7	50	225	211	211	18	42	21	187	144	164	186	180
1	0	72	15	66	8	4	13	1	19	42	40	62	2	11	10	56	31	42	43	36
0	0	0	0	0	0	0	0	0	0	0	0	0	0	0	0	0	0	0	0	0
0	0	1	1	1	0	0	0	0	1	1	1	1	0	0	0	1	0	0	0	1
0	0	22	10	24	1	3	5	1	14	42	43	49	2	12	3	18	20	30	21	14
0	0	0	0	0	0	0	0	0	1	1	0	0	0	0	0	3	0	1	0	0
4	10	1	1	0	4	0	1	0	2	3	1	0	0	1	0	0	0	1	2	0
0	0	1	0	1	0	0	3	0	0	0	0	0	0	0	0	0	1	1	1	0
0	0	0	0	0	1	0	0	0	0	0	0	0	0	0	0	0	0	0	0	0
4	3	2	13	0	5	4	4	4	5	5	4	7	1	21	11	5	5	1	5	4
0	0	10	32	7	33	2	4	3	13	6	3	0	0	3	1	33	7	25	17	20
0	0	1	5	1	1	0	0	0	0	2	0	1	0	0	0	0	0	1	1	0
0	0	1	48	0	3	0	0	0	0	0	5	0	0	0	0	0	0	1	1	0
153	81	7	63	27	179	47	64	25	35	36	42	26	66	121	20	71	125	56	72	86
30	24	0	3	1	0	16	19	15	10	1	0	1	0	0	23	0	0	0	0	0
18	15	1	15	2	32	3	1	3	3	6	7	11	16	14	5	3	7	3	7	6
5	17	10	58	15	19	3	12	10	13	10	5	5	3	2	2	5	13	5	3	4
17	15	16	12	1	34	2	3	3	2	15	13	11	52	22	3	4	10	10	15	9
43	24	2	20	5	0	3	8	3	7	0	0	0	68	17	11	4	20	24	15	25
92	75	0	14	5	2	1	3	5	4	1	0	1	11	23	19	2	0	6	0	3
2	8	3	26	7	46	27	23	12	22	4	25	14	5	16	8	5	8	29	11	8
11	109	0	0	0	0	0	0	0	0	0	0	0	35	4	1	1	1	0	0	1
1	12	0	0	0	0	0	0	0	0	0	0	0	84	36	0	1	0	0	0	1
0	0	1	0	0	0	0	0	0	0	0	0	0	0	0	0	1	0	0	0	1
2	0	0	0	0	0	0	0	0	0	0	0	0	32	49	37	0	0	0	0	1
0	0	0	0	0	0	0	0	0	0	0	0	0	1	6	0	0	0	0	0	0
0	0	0	0	0	0	0	0	0	0	0	0	0	0	0	0	0	1	0	0	0
8	0	4	0	0	0	27	5	97	8	0	0	0	0	0	26	0	4	0	0	0
0	0	2	0	0	0	4	2	1	2	0	0	0	0	0	2	0	0	0	0	0
0	0	1	0	0	0	1	1	0	0	0	0	0	0	0	0	0	0	0	0	0
0	0	0	0	0	0	0	0	0	0	0	0	0	0	0	0	0	0	0	0	0
0	0	0	0	0	0	0	0	0	0	0	0	0	0	0	0	0	0	0	0	0
0	0	1	0	0	0	1	1	0	0	0	0	0	0	0	2	0	0	0	0	0
0	0	0	0	0	0	0	0	0	0	0	0	0	0	0	0	0	0	0	0	0
0	0	0	0	0	0	0	0	0	0	0	0	0	0	0	0	0	0	0	0	0
0	0	0	0	0	0	0	0	0	0	0	0	0	0	0	0	0	0	0	0	0
0	0	0	0	0	0	0	0	0	0	0	0	0	0	0	0	0	0	0	0	0
0	0	0	0	0	0	2	0	2	0	0	0	0	0	0	1	0	0	0	0	0
0	0	0	0	0	0	0	0	1	0	0	0	0	0	0	0	0	0	0	0	0
0	0	0	0	0	0	1	0	0	0	0	0	0	0	0	0	0	0	0	0	0
0	0	0	0	0	0	0	0	0	0	0	0	0	0	0	0	0	0	0	0	0
0	0	0	0	0	0	12	2	7	0	0	0	0	0	0	1	0	0	0	0	0
0	0	0	0	0	0	4	1	5	0	0	0	0	0	0	0	0	0	0	0	0
0	0	0	0	0	0	0	0	1	0	0	0	0	0	0	0	0	0	0	0	0
0	0	0	0	0	0	3	0	1	1	0	0	0	0	0	0	0	0	0	0	0
0	0	0	0	0	0	6	0	2	0	0	0	0	0	0	2	0	0	0	0	0
0	0	0	0	0	0	7	0	2	0	0	0	0	0	0	1	0	0	0	0	0
0	0	0	0	0	0	2	2	2	0	0	0	0	0	0	4	0	0	0	0	0
0	0	0	0	0	0	6	0	0	0	0	0	0	0	0	0	0	0	0	0	0
0	0	0	0	0	0	0	0	0	0	0	0	0	0	0	0	0	0	0	0	0
0	0	0	0	0	0	0	0	0	0	0	0	0	0	0	0	0	0	0	0	0
0	0	0	0	0	0	0	0	0	0	0	0	0	0	0	0	0	0	0	0	0
0	0	0	0	0	0	0	0	0	0	0	0	0	0	0	0	0	0	0	0	0
0	0	0	0	0	0	0	0	0	0	0	0	0	0	0	0	0	0	0	0	0
0	0	0	0	0	0	0	0	0	0	0	0	0	0	0	0	0	0	0	0	0
0	0	0	0	0	0	0	0	0	0	0	0	0	0	0	0	0	0	0	0	0
0	0	0	0	0	0	0	0	0	0	0	0	0	0	0	0	0	0	0	0	0
0	0	0	0	0	0	1	0	1	0	0	0	0	0	0	1	0	0	0	0	0
0	0	0	0	0	0	2	0	2	0	0	0	0	0	0	0	0	0	0	0	0
394	400	400	400	400	400	215	216	220	210	400	400	400	398	400	223	400	400	400	400	400

(continued on next page)

Appendix A (*continued*)

Fine Fraction (0.25 0.125mm)

	CU-13	CU-14[a]	CU-15	CU-16	CU-17	CU-18	CU-19	CU-21	CU-22	CU-23	CU-42	MA-11	MA-12	MA-13	MA-14	MA-15	MA-31	MA-32	MA-33	MA-34
Qs	16		211	268	216	117	291	241	211	116	25	125	189	200	213	188	27	44	52	12
Qp	6		48	38	34	26	74	48	31	23	2	15	26	34	24	32	4	6	7	1
Qi	0		0	0	1	0	0	0	0	0	0	0	0	0	0	3	0	0	0	1
Qr	0		2	1	1	0	2	2	1	2	0	0	1	0	0	1	0	0	0	0
Ks	3		85	89	51	14	19	47	54	27	0	5	39	32	24	23	4	11	15	2
Kr	0		0	0	1	1	0	1	0	1	0	0	1	0	0	1	0	0	0	0
Mf	0		5	0	4	6	17	41	12	8	14	3	5	8	5	5	0	0	1	2
Ch	0		1	0	0	1	2	0	0	0	5	0	0	1	0	0	0	0	0	0
Mc	0		0	0	0	0	0	0	0	0	0	0	0	0	0	0	0	0	0	0
Ot	0		5	3	13	5	12	20	13	17	8	4	9	10	16	20	1	1	3	0
Sc	0		4	0	0	0	0	0	0	0	0	0	0	0	0	0	0	0	0	0
Sf	0		0	0	0	0	1	0	0	0	0	0	0	0	0	0	0	0	0	0
Sm	0		0	0	0	0	0	0	0	0	0	0	0	0	0	0	0	0	0	0
Lm	1		2	1	7	14	0	5	45	129	103	94	50	22	24	20	41	56	18	8
Lmb	0		0	0	0	1	0	0	1	4	8	16	1	0	0	0	20	17	0	3
Lmr	0		0	0	0	0	0	0	0	5	6	11	0	0	0	0	3	4	0	1
Lg	0		0	0	0	1	0	0	0	1	0	3	1	0	0	1	0	3	0	0
Le	0		2	0	3	2	1	1	10	39	73	34	12	4	5	7	23	40	7	11
Lc	0		3	1	12	8	2	9	23	44	131	27	12	4	10	7	75	93	22	26
Fe	0		2	0	0	0	0	0	3	4	5	8	3	1	0	2	11	6	1	0
Ls	0		2	0	1	0	0	1	0	1	2	5	1	0	1	1	2	3	0	0
Dm	0		0	0	4	2	1	4	2	0	5	7	2	4	11	11	8	6	3	6
De	0		3	1	5	3	4	2	1	1	2	2	7	8	16	14	10	5	12	2
Dc	1		20	12	30	49	2	11	21	0	28	14	15	53	66	61	143	87	55	48
Dd	0		1	2	7	1	0	0	1	0	10	2	3	3	4	3	28	19	7	0
Ds	0		1	0	2	2	0	2	1	0	0	0	1	0	0	0	1	0	1	0
Bio	2		0	0	1	0	0	0	0	0	0	0	0	0	0	0	0	0	0	0
In	416		16	12	47	149	0	1	8	17	12	122	48	39	26	20	10	16	207	352
XQm	3		5	0	3	20	0	0	0	1	0	1	0	0	0	0	0	0	17	0
XQp	0		1	0	3	6	0	0	0	0	0	0	0	0	1	1	0	0	0	0
XQi	0		0	0	0	0	0	0	0	0	0	0	0	0	0	0	0	0	0	0
XQr	0		0	0	0	0	0	0	0	0	0	0	0	0	0	0	0	0	0	0
XKs	2		2	0	0	3	0	0	0	0	0	0	1	0	0	0	0	0	1	0
XKr	0		0	0	0	0	0	0	0	0	0	0	0	0	0	0	0	0	0	0
XMf	0		0	0	0	0	0	0	0	0	0	0	0	0	0	0	0	0	0	0
XCh	0		0	0	0	0	0	0	0	0	0	0	0	0	0	0	0	0	0	0
XMc	0		0	0	0	0	0	0	0	0	0	0	0	0	0	0	0	0	0	0
XOt	0		0	0	0	1	0	0	0	0	0	0	0	0	0	0	0	0	0	1
XSc	0		0	0	0	0	0	0	0	0	0	0	0	0	0	0	0	0	0	0
XSf	0		0	0	0	0	0	0	0	0	0	0	0	0	0	0	0	0	0	0
XSm	0		0	0	0	0	0	0	0	0	0	0	0	0	0	0	0	0	0	0
XLm	0		0	0	0	2	0	0	0	0	0	0	0	0	0	0	0	0	2	1
XLm	0		0	0	0	0	0	0	0	0	0	0	0	0	0	0	0	0	0	0
XLmr	0		0	0	0	0	0	0	1	0	0	0	0	0	0	0	0	0	0	0
XLg	0		0	0	0	0	0	0	0	0	0	0	0	0	0	0	0	0	0	0
XLe	0		0	0	0	2	0	0	0	0	0	0	0	0	0	0	0	0	0	2
XLc	1		0	0	0	3	0	0	0	0	0	0	0	0	0	0	0	0	1	3
XFe	0		0	0	0	1	0	0	0	0	0	0	0	0	0	0	0	0	0	2
XLs	0		0	0	0	0	0	0	0	0	0	0	0	0	0	0	0	0	0	0
XDm	0		0	0	0	0	0	0	0	0	0	0	0	0	0	0	0	0	0	0
XDe	0		0	0	0	1	0	0	0	0	0	0	0	0	0	0	0	0	3	0
XDc	1		1	0	0	16	0	0	0	0	0	1	1	2	0	0	0	0	14	25
XDd	0		0	0	0	0	0	0	0	0	0	0	0	0	0	0	0	0	1	0
XDs	0		0	0	0	0	0	0	0	0	0	0	0	0	0	0	0	0	0	0
XBio	0		0	0	0	0	0	0	0	0	0	0	0	0	0	0	0	0	0	0
XIn	4		0	0	0	1	0	0	0	0	0	5	1	0	0	1	0	0	0	5
En	0		0	0	0	3	0	0	0	0	0	0	0	0	0	0	0	0	1	5
Total	456		422	428	446	461	428	436	440	442	439	504	429	435	446	422	411	417	451	519

[a] Non-available sand from this fraction.

MA-35	MA-42	MA-43	MA-44	MA-45	MA-46S	CÑ-21	CÑ-21S	-11	FU-12	-31	FU-41	FU-43	-45ª	FU-46	FU-410	FU-411	FU-411S	TR-31	TR-41
23	127	164	33	0	1	31	180	263	14	146	30	46	52	140	178	269	45	10	
4	19	24	6	0	1	1	19	42	1	20	5	6	7	13	53	43	13	3	
0	0	0	0	0	0	0	0	0	0	0	0	0	1	0	0	1	0	0	
0	2	0	0	0	0	0	1	4	0	0	0	0	0	0	2	2	0	0	
1	40	33	2	1	0	1	62	72	0	11	4	9	7	39	31	45	12	0	
0	1	1	0	0	0	0	2	1	0	0	0	1	0	0	0	1	0	0	
0	16	4	14	1	0	0	2	1	2	0	1	5	1	1	2	7	0	14	
0	0	2	0	0	1	0	0	0	0	0	0	1	0	0	2	0	0	0	
0	0	0	0	0	0	0	0	0	0	0	0	0	0	0	0	0	1	0	
1	71	8	5	0	0	1	6	1	2	5	1	4	2	7	2	1	1	13	
0	0	0	0	0	0	0	0	0	0	0	0	0	0	0	0	0	0	0	
0	0	0	0	0	0	0	0	0	0	0	0	0	0	0	0	0	0	0	
0	0	0	0	0	0	0	0	0	0	0	0	0	1	0	0	0	0	0	
14	25	20	62	51	30	1	29	1	5	49	7	7	4	5	1	0	20	148	
0	2	1	0	34	45	0	10	0	0	0	0	0	0	0	0	0	2	41	
2	0	0	2	0	0	0	0	0	0	1	0	0	0	0	0	0	0	3	
0	0	0	4	2	1	0	0	0	0	1	0	0	0	0	0	0	4	8	
11	8	4	37	0	3	0	7	7	11	24	7	10	14	2	2	0	34	26	
45	18	10	80	6	7	3	11	8	36	28	17	22	20	7	1	0	54	58	
0	3	0	5	7	8	0	4	0	0	0	4	3	0	1	0	0	2	39	
0	0	0	0	0	0	0	1	0	1	2	0	0	0	0	0	0	0	1	
27		13	19	5	2	1	1	1	17	7	1	7	9	4	8	1	1	13	
33	6	19	8	19	15	0	1	1	27	11	4	1	25	8	9	0	6	2	
164	53	109	105	270	296	3	27	11	293	43	18	31	261	65	112	52	61	2	
17	1	6	11	8	5	1	0	0	13	8	0	1	1	2	0	0	5	5	
1	1	0	0	0	0	0	0	0	1	0	0	0	0	0	0	0	0	0	
0	0	0	0	0	0	2	0	0	0	0	1	0	0	0	0	0	0	0	
68	79	35	51	6	2	451	57	1	5	71	287	260	25	134	15	0	205	30	
2	7	0	0	0	0	1	20	0	0	9	18	6	0	16	1	0	0	0	
0	0	0	0	0	0	0	3	0	0	2	2	0	0	3	0	0	0	0	
0	0	0	0	0	0	0	0	0	0	0	0	0	0	0	0	0	0	0	
0	0	0	0	0	0	0	0	0	0	0	0	0	0	0	0	0	0	0	
1	1	0	0	0	0	1	9	0	0	0	2	2	0	4	0	0	1	1	
0	0	0	0	0	0	0	0	0	0	0	0	0	0	0	0	0	0	0	
0	0	0	0	0	0	0	0	0	0	0	0	1	0	0	0	0	0	0	
0	0	0	0	0	0	0	0	0	0	0	0	0	0	0	0	0	0	0	
0	0	0	0	0	0	0	0	0	0	0	0	0	0	0	0	0	0	0	
0	1	0	0	0	0	0	1	0	0	0	0	1	0	0	0	0	0	0	
0	0	0	0	0	0	0	0	0	0	0	0	0	0	0	0	0	0	0	
0	0	0	0	0	0	0	0	0	0	0	0	0	0	0	0	0	0	0	
0	0	0	0	0	0	0	0	0	0	0	0	0	0	0	0	0	0	0	
0	0	0	0	0	0	0	0	0	0	0	0	0	0	0	0	0	0	0	
0	0	0	0	0	0	0	0	0	0	0	0	0	0	0	0	0	0	0	
0	0	0	0	0	0	0	0	0	0	0	0	0	0	0	0	0	0	0	
0	0	0	0	0	0	0	0	0	0	0	0	0	0	0	0	0	0	0	
0	0	0	0	0	0	0	0	0	0	0	0	0	0	0	0	0	0	0	
0	0	0	0	0	0	0	0	0	0	0	0	0	0	0	0	0	0	0	
0	0	0	0	0	0	0	0	0	0	0	0	0	0	0	0	0	0	0	
0	0	0	0	0	0	0	0	0	0	0	0	0	0	0	0	0	0	0	
0	0	0	0	0	0	0	0	0	0	0	0	0	0	0	0	0	0	0	
0	0	0	0	0	0	0	0	0	0	0	0	0	0	0	0	0	0	0	
0	0	0	0	0	0	0	0	0	0	0	0	0	0	0	0	0	0	0	
0	0	0	0	0	0	0	0	0	0	0	0	0	0	0	0	0	0	0	
0	0	0	0	0	0	0	0	0	0	0	0	0	0	0	0	0	0	0	
0	0	0	0	0	0	0	0	0	0	0	0	0	0	0	0	0	0	0	
0	0	0	0	0	0	0	0	0	0	0	0	0	0	0	0	0	0	0	
0	0	0	0	0	0	0	0	0	0	0	0	0	0	0	0	0	0	0	
0	0	0	0	0	0	0	0	0	0	0	0	0	0	0	0	0	0	0	
0	0	0	0	0	0	0	0	0	0	0	0	0	0	0	0	0	0	0	
0	0	0	0	0	0	0	0	0	0	0	0	0	0	0	0	0	0	0	
0	0	0	0	0	0	0	0	0	0	0	0	0	0	0	0	0	0	0	
1	0	0	0	0	0	0	0	0	0	0	4	2	0	1	0	0	0	1	
1	1	0	0	0	0	0	6	0	0	0	7	5	0	5	0	0	5	2	
0	0	0	0	0	0	0	0	0	0	0	0	1	0	0	0	0	0	1	
0	0	0	0	0	0	0	0	0	0	0	0	0	0	0	0	0	0	0	
0	0	0	0	0	0	0	0	0	0	0	2	0	0	0	0	0	0	0	
0	1	0	0	0	0	0	0	0	0	1	2	0	1	0	0	0	0	0	
7	9	1	0	0	0	1	1	0	2	1	12	4	2	6	0	0	0	0	
0	0	0	0	0	0	0	0	0	0	0	0	0	0	0	0	0	0	0	
0	0	0	0	0	0	0	0	0	0	0	0	0	0	0	0	0	0	0	
0	0	0	0	0	0	0	0	0	0	0	0	0	0	0	0	0	0	0	
0	0	0	0	0	0	2	0	0	0	0	0	0	0	0	0	0	1	0	
0	2	0	0	0	0	0	4	0	0	0	1	0	0	1	0	0	0	0	
429	496	454	444	410	417	503	466	420	428	440	439	440	435	466	419	426	475	425	

(continued on next page)

Appendix A (*continued*)

	TR-42	TR-43	TR-44S	TR-45S	TE-11	TE-12	TE-12S	TE-13	TE-14	TE-15	TE-16	TE-31	TE-32	TE-33	TE-34	TE-35	TE-35S	TE-36	TE-37	TE-37S
Qs	27	228	162	239	93	55	116	40	128	203	185	216	37	81	55	214	163	186	212	194
Qp	2	55	34	69	15	10	44	11	38	39	38	30	8	12	9	57	38	58	56	42
Qi	0	0	0	0	0	0	0	0	0	0	0	0	0	0	0	0	0	0	0	0
Qr	0	4	1	2	0	0	0	0	0	1	0	0	0	0	0	1	3	2	2	1
Ks	4	38	52	64	16	13	46	13	69	71	61	50	6	24	18	63	73	68	58	48
Kr	0	2	0	0	0	0	0	0	1	1	0	0	0	0	0	0	1	1	2	0
Mf	24	5	6	2	5	1	8	3	2	0	0	2	0	5	1	0	2	0	0	0
Ch	0	0	0	1	1	1	0	1	1	0	0	1	0	0	1	1	1	0	3	0
Mc	0	0	2	0	0	0	0	0	0	0	0	0	0	0	0	1	0	0	0	0
Ot	4	5	14	6	7	9	10	7	5	15	7	16	5	15	12	6	4	5	6	10
Sc	2	3	11	2	31	5	2	3	8	2	6	2	0	3	0	2	2	8	7	15
Sf	0	0	1	0	0	0	0	0	0	0	0	0	0	0	0	0	0	0	1	0
Sm	0	2	3	0	0	0	0	0	1	0	0	0	0	0	0	0	0	0	1	0
Lm	66	14	31	12	106	105	95	67	93	47	64	53	42	98	140	44	65	45	28	49
Lmb	31	2	12	2	13	9	9	15	8	5	6	7	13	35	38	5	7	5	3	3
Lmr	6	1	3	0	6	0	1	5	1	1	3	2	0	1	4	0	0	0	0	1
Lg	22	5	18	3	19	17	7	2	11	6	13	5	1	11	3	1	6	3	6	6
Le	25	10	8	6	34	10	12	14	3	3	4	5	18	24	28	0	3	5	3	4
Lc	41	5	23	3	12	11	13	22	10	6	6	6	105	41	25	3	22	22	12	18
Fe	60	1	9	4	5	3	4	1	4	1	3	2	9	21	16	0	4	0	1	2
Ls	3	5	13	3	33	12	11	8	17	8	4	14	2	4	6	1	8	7	4	4
Dm	80	1	0	0	0	0	0	1	2	1	0	0	35	3	4	1	0	2	2	3
De	3	0	0	0	1	0	0	0	0	0	0	0	44	3	5	0	1	0	1	0
Dc	4	2	1	2	0	0	0	0	0	0	0	0	8	9	10	7	2	2	8	1
Dd	16	0	0	0	0	0	2	0	0	1	0	0	85	24	26	0	0	1	0	1
Ds	1	0	0	0	0	0	0	0	0	0	0	0	2	1	0	2	0	1	1	2
Bio	0	0	0	0	0	0	0	1	0	0	0	0	0	0	0	0	0	0	0	0
In	12	4	7	0	9	176	21	256	12	5	4	1	1	3	44	4	8	1	1	3
XQm	0	11	0	0	2	7	7	1	0	2	2	3	0	0	2	1	0	0	0	1
XQp	0	4	0	0	0	3	2	1	1	0	0	2	0	0	0	0	0	0	0	0
XQi	0	0	0	0	0	0	0	0	0	0	0	0	0	0	0	0	0	0	0	0
XQr	0	0	0	0	0	0	0	0	0	0	0	0	0	0	0	0	0	0	0	0
XKs	0	10	0	0	1	2	3	2	1	0	1	2	0	0	0	0	0	0	1	0
XKr	0	0	0	0	0	0	0	0	0	0	0	0	0	0	0	0	0	0	0	0
XMf	0	0	0	0	0	0	0	0	0	0	0	0	0	0	0	0	0	0	0	0
XCh	0	0	0	0	0	0	0	0	0	0	0	0	0	0	0	0	0	0	0	0
XMc	0	0	0	0	0	0	0	0	0	0	0	0	0	0	0	0	0	0	0	0
XOt	0	0	0	0	0	3	0	1	0	0	0	0	0	0	0	0	0	0	0	0
XSc	0	0	0	0	0	1	0	0	0	0	0	0	0	0	0	0	0	0	0	0
XSf	0	0	0	0	0	0	0	0	0	0	0	0	0	0	0	0	0	0	0	0
XSm	0	0	0	0	0	0	0	0	0	0	0	0	0	0	0	0	0	0	0	0
XLm	0	0	0	0	0	22	0	8	0	0	0	0	0	0	0	0	0	0	0	0
XLm	0	0	0	0	0	0	0	0	0	0	0	0	0	0	0	0	0	0	0	0
XLmr	0	0	0	0	0	0	0	0	0	0	0	0	0	0	0	0	0	0	0	0
XLg	0	0	0	0	0	0	0	0	0	0	0	0	0	0	0	0	0	0	0	0
XLe	0	0	0	0	1	2	0	0	0	0	0	0	0	0	0	0	0	0	0	0
XLc	1	0	0	0	0	2	0	5	0	0	1	0	0	0	0	0	0	0	0	0
XFe	0	0	0	0	0	0	0	0	0	0	0	0	0	0	0	0	0	0	0	0
XLs	0	0	0	0	0	1	0	0	0	0	0	0	0	0	0	0	0	0	0	0
XDm	0	0	0	0	0	0	0	0	0	0	0	0	0	0	0	0	0	0	0	0
XDe	0	0	0	0	0	0	0	0	0	0	0	0	0	0	0	0	0	0	0	0
XDc	0	0	0	0	0	0	0	0	0	0	0	0	0	0	0	0	0	0	0	0
XDd	0	0	0	0	0	0	0	0	0	0	0	0	0	0	0	0	0	0	0	0
XDs	0	0	0	0	0	0	0	0	0	0	0	0	0	0	0	0	0	0	0	0
XBio	0	0	0	0	0	0	0	0	0	0	0	0	0	0	0	0	0	0	0	0
Xln	0	0	0	0	0	1	0	0	0	0	0	0	0	0	1	0	0	0	0	0
En	0	2	0	0	0	1	0	2	0	0	0	0	0	0	0	0	0	0	0	0
Total	431	415	411	420	410	482	413	490	416	418	408	419	421	418	448	414	413	422	419	408

Appendix B. Quantification of lithologies and slope at the sources

	CU-13		CU-14		CU-15		CU-16		CU-17		CU-18		CU-19		CU-21		CU-22		CU-23		CU-42		MA-11		MA-12		MA-13		MA-14	
	%	Slp[a]	%	Slp	%	Slp	%	Slp	%	Slp	%	Slp	%	Slp	%	Slp	%	Slp	%	Slp	%	Slp	%	Slp	%	Slp	%	Slp	%	Slp
Lmwp	12.1	21.5	12.9	21.2	14.9	19.5	13.9	22.3	11.4	21.4	10.6	16.8	11.9	20.1	28.7	14.3	38.2	14.2	10.1	4.9	0.0		25.2	8.3	22.5	29.0	12.2	15.4	13.0	19.0
Lgec	0.3	9.6	0.4	9.6	0.0		0.0		0.8	9.6	0.0		0.9	7.9	21.9	10.7	26.2	11.1	28.2	10.2	0.0		0.0		0.4	36.8	0.9	13.3	1.0	15.8
Dm	12.7	37.5	13.3	36.7	17.3	32.3	17.6	31.9	13.4	40.5	14.9	50.4	14.3	39.2	4.8	26.2	0.3	31.4	0.4	45.0	0.0		13.7	33.7	14.3	31.4	36.5	25.1	36.1	27.0
Dr	27.3	20.5	22.3	14.3	19.8	12.6	30.1	13.5	24.6	15.0	43.0	21.3	12.0	22.1	23.2	11.1	26.2	11.1	28.2	10.3	100.0	20.5	24.8	31.8	23.1	30.9	34.0	26.8	33.2	28.3
AN	23.2	21.3	26.1	21.3	21.3	22.7	13.6	26.3	25.5	22.1	10.7	24.3	31.2	22.7	9.6	16.6	3.5	9.4	15.9	6.6	0.0		15.6	30.2	17.6	29.3	0.9	11.4	1.9	30.2
Mar	24.3	27.4	24.9	26.8	26.6	27.1	24.7	29.4	24.2	29.3	20.7	41.1	29.6	28.4	11.7	16.9	5.5	10.5	17.1	6.3	0.0		20.6	23.6	22.0	28.0	15.5	21.5	14.7	23.4

	MA-15		MA-31		MA-32		MA-33		MA-34		MA-35		MA-42		MA-43		MA-44		MA-45		MA-46S		CÑ-21		CÑ-21S		FU-11		FU-12	
	%	Slp	%	Slp	%	Slp	%	Slp	%	Slp	%	Slp	%	Slp	%	Slp	%	Slp	%	Slp	%	Slp	%	Slp	%	Slp	%	Slp	%	Slp
Lmwp	12.2	19.0	0.0		0.0		0.0		0.0		0.0		25.3	15.7	11.7	13.9	0.0		0.0		0.0		17.7	25.6	17.7	25.6	0.0		0.0	
Lgec	0.8	15.8	0.0		0.0		0.0		0.0		0.0		0.0		0.5	10.1	0.0		0.0		0.0		9.9	27.6	9.9	27.6	10.9	28.9	12.0	17.7
Dm	35.4	27.4	35.5	24.8	36.0	20.4	17.7	19.9	22.1	22.2	20.3	21.5	19.8	20.4	37.5	16.5	39.6	19.1	15.1	8.2	15.3	8.5	4.2	31.1	4.2	31.1	0.6	6.9	5.2	54.0
Dr	34.1	29.0	53.2	24.1	50.8	19.1	50.1	17.7	55.3	18.8	51.5	19.1	20.8	21.2	28.2	17.1	50.6	17.7	45.7	8.2	47.0	8.5	43.0	31.5	43.0	31.5	87.5	32.8	75.4	24.3
AN	2.3	31.6	0.0		0.0		13.0	19.7	0.0		0.0		8.0	32.6	7.0	36.9	0.0		0.0		0.0		13.3	18.6	13.3	18.6	0.0		0.0	
Mar	15.1	24.4	11.2	23.3	13.1	14.7	19.1	20.3	22.5	20.9	28.1	16.2	26.0	18.5	15.0	19.1	9.7	12.0	39.1	8.1	37.6	8.6	11.8	21.8	11.8	21.8	0.9	6.9	7.3	54.0

	FU-31		FU-41		FU-43		FU-45		FU-46		FU-410		FU-411		FU-411S		TR-31		TR-41		TR-42		TR-43		TR-44S		TR-45S		TE-11	
	%	Slp	%	Slp	%	Slp	%	Slp	%	Slp	%	Slp	%	Slp	%	Slp	%	Slp	%	Slp	%	Slp	%	Slp	%	Slp	%	Slp	%	Slp
Lmwp	14.5	15.3	20.9	17.2	21.9	12.3	13.9	25.1	7.2	22.9	10.7	20.9	6.6	18.6	6.6	18.6	3.5	14.4	74.2	19.8	51.9	26.5	9.8	9.9	59.0	13.2	50.4	13.6	40.6	13.3
Lgec	3.0	38.3	5.1	39.7	4.5	1.6	2.9	36.8	2.4	34.3	5.9	41.5	7.4	41.7	7.4	41.7	0.0		14.4	19.4	10.1	24.8	49.1	14.8	18.3	18.2	25.1	19.3	21.8	9.4
Dm	4.0	26.2	1.0	51.5	0.0		12.0	22.1	26.8	20.3	8.3	36.3	5.9	40.6	5.9	40.6	1.5	21.1	1.8	25.6	0.2	25.3	0.0		0.0		0.0		9.3	10.0
Dr	33.3	33.3	54.8	39.9	68.9	25.0	53.0	34.3	63.2	28.3	48.3	40.7	43.2	37.9	43.2	37.9	74.1	21.5	0.0		0.0		0.0		0.0		0.0		0.0	
AN	20.0	28.0	10.0	49.6	0.9	15.9	13.1	40.4	0.0		16.1	36.4	29.9	25.9	29.9	25.9	0.0		0.0		7.0	23.9	25.6	14.4	6.5	23.2	10.7	21.7	23.3	3.4
Mar	25.1	25.3	8.1	25.5	3.7	34.1	5.0	41.9	0.3	13.2	10.6	36.5	6.9	37.6	6.9	37.6	20.8	23.0	9.5	34.0	30.7	29.8	15.4	10.2	16.1	19.1	13.7	19.0	4.9	19.0

	TE-12		TE-12S		TE-13		TE-14		TE-15		TE-16		TE-31		TE-32		TE-33		TE-34		TE-35		TE-35S		TE-36		TE-37		TE-37S	
	%	Slp	%	Slp	%	Slp	%	Slp	%	Slp	%	Slp	%	Slp	%	Slp	%	Slp	%	Slp	%	Slp	%	Slp	%	Slp	%	Slp	%	Slp
Lmwp	40.5	20.8	40.5	20.8	39.9	18.5	40.9	25.5	28.6	29.0	34.5	26.2	21.7	21.2	4.5	15.7	6.3	16.0	5.8	15.3	30.6	31.2	30.6	31.2	30.7	33.4	26.8	32.3	26.8	32.3
Lgec	13.2	13.9	13.2	13.9	15.1	12.0	13.8	20.1	11.0	22.7	12.3	19.5	6.9	22.5	3.2	23.6	4.5	24.0	4.2	23.0	11.2	25.4	11.2	25.4	9.6	29.1	9.1	27.2	9.1	27.2
Dm	3.8	22.7	3.8	22.7	5.2	16.1	7.3	22.5	4.4	24.8	5.8	21.8	2.3	21.8	0.0		0.0		0.0		5.3	28.9	5.3	28.9	4.9	32.2	4.5	30.6	4.5	30.6
Dr	4.8	11.9	4.8	11.9	3.3	12.3	0.0		0.3	19.0	0.2	19.0	21.7	8.5	83.1	9.9	76.3	11.7	78.1	11.7	0.0		0.0		1.0	32.2	0.6	30.3	0.6	30.3
AN	12.0	15.4	12.0	15.4	15.4	12.1	21.0	18.4	43.3	20.6	32.6	19.2	34.2	24.1	3.4	23.6	4.9	24.0	4.5	23.0	36.4	24.6	36.4	24.6	31.8	28.5	38.1	24.3	38.1	24.3
Mar	25.6	30.5	25.6	30.5	21.0	27.4	16.9	29.3	12.3	28.8	14.5	28.9	13.1	20.9	5.7	23.6	7.9	24.0	7.3	23.0	16.4	29.1	16.4	29.1	21.9	30.9	20.8	26.0	20.8	26.0

[a] Slp: Slope percentage.

References

Alvaro, M., Capote, R., Vegas, R., 1979. Un modelo de evolución geotectónica para la Cadena Celtibérica. Acta Geol. Hisp. 14, 172–177.

Arribas, M.E., Tortosa, A., 1998. Coeval carbonate grains in modern fluvial sands (Iberian Range, Spain): the activity of a continental carbonate factory. In: Cañaveras, J.C., García del Cura, M.A., Soria, J. (Eds.), Abstracts of the 15th International Sedimentological Conference, Alicante, Spain, p. 154.

Arribas, J., Gómez-Gras, D., Rosell, J., Tortosa, A., 1990. Estudio comparativo entre las areniscas Paleozoicas y Triásicas de la isla de Menorca: evidencias de procesos de reciclado. Rev. Soc. Geol. Esp. 3, 105–116.

Arribas, J., Critelli, S., Le Pera, E., Tortosa, A., 2000. Composition of modern stream sand derived from a mixture of sedimentary and metamorphic source rocks (Henares River Central Spain). Sediment. Geol. 133, 27–48.

Basu, A., 1985. Influence of climate and relief on compositions of sands released at source areas. In: Zuffa, G.G. (Ed.), Provenance of Arenites. Reidel, Dordrecht, pp. 1–18.

Basu, A., Young, S.W., Suttner, L.J., James, W.C., Mack, G.H., 1975. Re-evaluation of the use of undulatory extinction and polycrystallinity in detrital quartz for provenance interpretation. J. Sediment. Petrol. 45, 873–882.

Bathurst, R.G.C., 1975. Carbonate Sediments and Their Diagenesis. Elsevier, Amsterdam, 658 pp.

Blatt, H., Jones, R.L., 1975. Proportions of exposed igneous, metamorphic, and sedimentary rocks. Geol. Soc. Amer. Bull. 86, 1085–1088.

Blatt, H., Middleton, G.V., Murray, R.C., 1980. Origin of Sedimentary Rocks. Prentice-Hall, New Jersey, 634 pp.

Cavazza, W., Zuffa, G.G., Camporesi, C., Ferretti, C., 1993. Sedimentary recycling in a temperate climate drainage basin (Senio River, north-central Italy): composition of source rock, soil profiles, and fluvial deposits. In: Johnsson, M.J., Basu, A. (Eds.), Processes Controlling the Composition of Clastic Sediments. Geol. Soc. Am. Special Paper, vol. 284, pp. 247–261.

Chave, K.E., Schmalz, R.F., 1966. Carbonate-seawater reactions. Geochim. Cosmochim. Acta 30, 1037–1048.

Chayes, F., 1952. Notes on the staining of potash feldspar with sodium cobaltinitrite in thin section. Am. Mineral. 37, 337–340.

Dickinson, W.R., 1970. Interpreting detrital modes of graywacke and arkose. J. Sediment. Petrol. 40, 695–707.

Dickinson, W.R., 1985. Interpreting provenance relations from detrital modes of sandstones. In: Zuffa, G.G. (Ed.), Provenance of Arenites. Reidel, Dordrecht, pp. 333–362.

Dickinson, W.R., Suczek, C.A., 1979. Plate tectonics and sandstone composition. AAPG Bull. 63, 2164–2182.

Dickinson, W.R., Beard, L.S., Brakenridge, G.R., Erjavec, J.L., Ferguson, R.C., Inman, K.F., Knepp, R.A., Lindberg, F.A., Ryberg, P.T., 1983. Provenance of north American phanerozoic sandstones in relation to tectonic setting. Geol. Soc. Amer. Bull. 94, 222–235.

Evamy, B.D., 1963. The application of chemical staining technique to a study of dedolomitization. Sedimentology 2, 164–170.

Fernández Calvo, C., 1981. Sedimentología y diagénesis del Cretácico Superior de La Mancha (Cuenca). PhD Thesis, Univ. Complutense, Madrid, 299 pp.

Folk, R.L., 1974. Petrology of Sedimentary Rocks. Hemphill Publishing, Austin, TX, 182 pp.

Freytet, P., Verrecchia, E.P., 1998. Freshwater organisms that build stromatolites: a synopsis of biocrystallization by prokaryotic and eukaryotic algae. Sedimentology 45, 535–563.

Garrels, R.M., 1986. Sediment cycling and diagenesis. U.S. Geol. Surv. Bull. 1578, 1–11.

Gazzi, P., 1966. Le arenarie del flysch sopracretaceo dell'Appennino modenese; correlazioni con il Flysch di Monghidoro. Mineral. Petrogr. Acta 12, 69–97.

Grantham, J.H., Velbel, M.A., 1988. The influence of climate and topography on rock-fragment abundance in modern fluvial sands of the southern Blue Ridge Mountains, North Carolina. J. Sediment. Petrol. 58, 219–227.

Ibbeken, H., Schleyer, R., 1991. Source and sediment. A Case Study of Provenance and Mass Balance at an Active Plate Margin (Calabria, Southern Italy). Springer-Verlag, Berlin, 286 pp.

I.G.N., 1991a. Atlas Nacional de España; II.9, Climatología, Instituto Geografico Nacional, Ministerio de Obras Públicas y Transportes (MOPT), Madrid, 24 pp.

I.G.N., 1991b. Atlas Nacional de España; II.7, Edafología, Instituto Geografico Nacional, Ministerio de Obras Públicas y Transportes (MOPT), Madrid, 14 pp.

Ingersoll, R.V., Bullard, T.F., Ford, R.L., Grimm, J.P., Pickle, J.D., Sares, S.W., 1984. The effect of grain size on detrital modes: a test of the Gazzi–Dickinson point-counting method. J. Sediment. Petrol. 54, 103–116.

Ingersoll, R.V., Kretchmer, A.G., Valles, P.K., 1993. The effect of sampling scale on actualistic sandstone petrofacies. Sedimentology 40, 937–953.

I.T.G.E., 1983a. Mapa Geológico de España. Escala 1/50.000. Hoja no. 589. Terriente. Memoria explicativa, 80 pp.

I.T.G.E., 1983b. Mapa Geológico de España. Escala 1/50.000. Hoja no. 565. Tragacete. Memoria explicativa, 89 pp.

I.T.G.E., 1986. Mapa Geológico de España. Escala 1/50.000. Hoja no. 611. Cañete. Memoria explicativa, 64 pp.

I.T.G.E., 1989a. Mapa Geológico de España. Escala 1/50.000. Hoja no. 610. Cuenca. Memoria explicativa, 56 pp.

I.T.G.E., 1989b. Mapa Geológico de España. Escala 1/50.000. Hoja no. 564. Fuertescusa. Memoria explicativa, 54 pp.

I.T.G.E., 1989c. Mapa Geológico de España. Escala 1/50.000. Hoja no. 587. Las Majadas. Memoria explicativa, 60 pp.

Johnsson, M.J., 1993. The system controlling the composition of clastic sediments. In: Johnsson, M.J., Basu, A. (Eds.), Processes Controlling the Composition of Clastic Sediments. Geol. Soc. Am. Special Paper, vol. 284, pp. 1–19.

Köppen, W., 1901. Versuch einer Klassifikation der klimate vorzugsweise nach ihren Beziehungen zur Pflanzenwelt. Geogr. Z. 6 (593 pp.).

Le Pera, E., Arribas, J., Critelli, S., Tortosa, A., 2001. The effects of source rocks and chemical weathering on the petrogenesis of siliciclastic sand from the Neto river (Calabria, Italy): implications for provenance studies. Sedimentology 48, 357–378.

Mack, G.H., 1981. Composition of modern stream sand in a humid climate derived from a low-grade metamorphic and sedimentary

foreland fold-thrust belt of north Georgia. J. Sediment. Petrol. 51, 1247–1258.

Montesinos, S., Arribas, J., 1998. Source area versus detrital products: a geographical information system approach. In: Cañaveras, J.C., García del Cura, M.A., Soria, J. (Eds.), Abstracts of the 15th International Sedimentological Conference, Alicante, Spain, pp. 558–559.

Moulton, K.L., Berner, R.A., 1998. Quantification of the effect of plants on weathering: studies in Iceland. Geology 26, 895–898.

Odom, I.E., Doe, T.W., Dott, R.H., 1976. Nature of feldspar–grain size relations in some quartz-rich sandstones. J. Sediment. Petrol. 46, 862–870.

Palomares, M., Arribas, J., 1993. Modern stream sands from compound crystalline sources: composition and sand generation index. In: Johnsson, M.J., Basu, A. (Eds.), Processes Controlling the Composition of Clastic Sediments. Geol. Soc. Am. Special Paper, vol. 284, pp. 313–322.

Pedley, H.M., 1990. Classification and environmental models of cool freshwater tufas. Sediment. Geol. 68, 143–154.

Potter, P.E., 1978. Petrology and chemistry of modern big river sands. J. Geol. 86, 423–449.

Potter, P.E., 1994. Modern sands of south America: composition, provenance and global significance. Geol. Rundsch. 83, 212–232.

Reeder, R.J., 1983. Crystal chemistry of the rhombohedral carbonates. Min. Soc. Am. Rev. Mineral. 11, 1–48.

Valloni, R., 1985. Reading provenance from modern marine sands. In: Zuffa, G.G. (Ed.), Provenance of Arenites. Reidel, Dordrecht, pp. 309–332.

Vilas, L., Mas, R., García, A., Arias, C., Alonso, A., Meléndez, N., Rincón, R., 1982. Ibérica suroccidental. El Cretácico de España. Univ. Complutense Madrid, Madrid, pp. 457–514.

Wilson, L., 1969. Les rélations entre les processus géomorphologiques et le climat moderne comme méthode de paléoclimatologie. Rev. Géogr. Phys. Géol. Dyn. 11, 303–314.

Zuffa, G.G., 1980. Hybrid arenites: their composition and classification. J. Sediment. Petrol. 50, 21–29.

Zuffa, G.G., 1987. Unravelling hinterland and offshore paleogeography from deep-water arenites. Deep-Marine Clastic Sedimentology. In: Leggett, J.K., Zuffa, G.G. (Eds.), Concepts and Case Studies. Graham and Trotman, London, pp. 39–61.